chemosensors

MDPI

Review

Recent Advances in Functionalization Strategies for Biosensor Interfaces, Especially the Emerging Electro-Click: A Review

Feiyu Wang, Yiwen Xie, Weijie Zhu and Tianxiang Wei *

School of Environment, Nanjing Normal University, Nanjing 210023, China; 212502033@njnu.edu.cn (F.W.); 222502041@njnu.edu.cn (Y.X.); 222512016@njnu.edu.cn (W.Z.)
* Correspondence: weitianxiang@njnu.edu.cn

Abstract: The functionalization of biosensor interfaces constitutes a crucial aspect of biosensing systems, as it directly governs key characteristics, including sensitivity, selectivity, accuracy, and rapidity. Among the diverse range of functionalization strategies available for biosensor interfaces, the click reaction has emerged as an exceptionally straightforward and stable approach for modifying electrodes and sensing films. Notably, the electro-click reaction enables the reagent-free functionalization of the biosensing interface, offering significant advantages, such as high speed, selectivity, and minimal pollution. Consequently, this strategy has garnered substantial attention and is widely regarded as a promising avenue for enhancing biosensor interface functionalization. Within this comprehensive review, we commence by presenting the latest advancements in functionalized biosensor interfaces, organizing the regulatory strategies into distinct categories based on the mediators employed, ranging from nanomaterials to biomolecules. Subsequently, we provide a comprehensive summary with an emphasis on recently developed electro-click strategies for functionalizing electrochemical and optical biosensor interfaces, covering both principles and applications. It is our anticipation that gaining a profound understanding of the principles and applications underlying electro-click strategies for biosensor interface functionalization will facilitate the design of highly selective and sensitive biosensor systems for diverse domains, such as clinical, pharmaceutical, environmental, and food analyses.

Keywords: biosensor; interface; functionalization; electro-click; electrochemistry

Citation: Wang, F.; Xie, Y.; Zhu, W.; Wei, T. Recent Advances in Functionalization Strategies for Biosensor Interfaces, Especially the Emerging Electro-Click: A Review. *Chemosensors* **2023**, *11*, 481. https://doi.org/10.3390/chemosensors11090481

Academic Editor: Camelia Bala

Received: 26 June 2023
Revised: 12 August 2023
Accepted: 24 August 2023
Published: 1 September 2023

1. Introduction

Biosensors represent a distinct branch within the broader domain of analytical sensors, with a specific emphasis on incorporating biometric entities into the detection mode [1]. These remarkable devices house miniature analytical sensing systems that seamlessly integrate biometric components, thereby showcasing micro-level analyte specificity. By leveraging this capability, biosensors can proficiently identify a diverse array of analytes, including proteins, cells, and viruses within living organisms, as well as track heavy-metal pollutants and biochemical waste within the environment encompassing air, water, and soil [2,3]. The accurate detection of these analytes assumes paramount importance in disease surveillance and treatment and environmental monitoring [4]. Typical biosensors contain two basic functional units: recognition elements and signal transducers [5]. The selectivity of a biosensor hinges upon the inherent properties of the recognition element, while its sensitivity relies upon the signal transducer. The fusion of these two components facilitates the attainment of stringent requirements for both high selectivity and sensitivity. The analysis process of a biosensor is usually carried out on the sensor interface. It is at this interface that the core functionality and defining characteristics of the biosensor, such as the sensitivity, selectivity, accuracy, and speed, are directly determined. Accordingly, the development of innovative interfaces stands as the foundational approach for enhancing the biosensor performance. Hence, the functionalization of biosensor interfaces assumes a vital role within the biosensing system.

Numerous studies have focused on the development of novel and improved materials for the functionalization of biosensor interfaces [6,7]. In addition, researchers have proposed more controllable, safe, and convenient strategies to enhance the efficiency of functionalization. In 2001, Professor Sharpless and his team introduced the concept of "Click Chemistry" along with a series of reactions aligned with this concept, marking its first introduction to the scientific community [8]. Despite being a relatively recent concept, click chemistry has gained widespread adoption in various fields, including biomolecular labeling and detection, biomolecular modification, drug lead-compound discovery, drug delivery, polymer modification, fluorescence imaging, CRISPR sgRNA synthesis, target gene labeling, and more. Notably, click chemistry has found significant application in the development of highly controllable, selective, and sensitive biosensing platforms [9–15]. It is worth mentioning that the 2022 Nobel Prize in Chemistry was jointly awarded to American chemist Carolyn Bertozzi, Danish chemist Morten Meldal, and American chemist Barry Sharpless for their contributions to the development of click chemistry and biological orthogonal chemistry.

In recent years, electrochemical reactions have garnered increasing attention due to their rapid reaction kinetics, relatively straightforward reaction conditions, and minimal environmental impact. This has led to the emergence of the electro-click method. Compared to traditional click reactions, the reagent-free nature of the electro-click method makes it a good candidate for functionalization strategies employed in biosensor interfaces [16]. In this paper, we present a comprehensive review of recent advancements in biosensor interface functionalization strategies, with a particular emphasis on the electro-click functionalization strategy. It is anticipated that this review will positively contribute to the development of more precise and high-performance biosensors through the utilization of the electro-click strategy.

2. Functionalization Technologies of Biosensor Interfaces

As previously mentioned, the fundamental components of typical biosensors are recognition elements and signal transducers. To imbue biosensors with specific functions and enhance their performance, it becomes necessary to functionalize the biosensing interface. In this context, nanostructures, macromolecules, small molecules, and cells assume crucial roles as regulators mediating the process of functionalization. Various strategies exist to modify these regulators onto the biosensor interface, including physical adsorption, covalent binding, redox reactions, electrostatic self-assembly, and more. These functionalization strategies empower biosensors to achieve efficient and specific target recognition, minimize background noise, and amplify sensing signals. In the subsequent discussion, we will delve into recent research advancements in this field.

2.1. Nanostructured Biosensor Interface

The integration of nanomaterials into the biosensor interface results in a nanostructured biosensor interface, thereby altering the chemical binding profile and composition of the sensing interface. This integration facilitates the attainment of unique detection modes, enhances sensitivity and specificity, and imparts novel properties to the entire biosensor system [17]. The interface between nanomaterials and biomolecules has played a pivotal role in the development of biosensors optimized for diverse objectives and applications.

2.1.1. Carbon Nanomaterials

Carbon nanomaterials, owing to their exceptional electrical conductivity, high stability, and ease of functionalization, have found extensive utilization in various biosensor interfaces [18].

Graphene Nanomaterials

Graphene, with its large specific surface area and excellent conductivity, has emerged as an ideal sensing surface that can be functionalized by grafting different functional

groups [19]. As a monolayer graphite with intriguing physical and chemical properties [20], graphene has been extensively employed in the construction of nanostructured biosensor interfaces, as highlighted in many research reviews [21–24].

Graphene oxide (GO) utilizes its high specific surface area to accommodate a greater number of recognition elements or employs its unique sp^2 structure to specifically adsorb corresponding molecules. Moreover, it enhances the performance of transducers by facilitating electron transfer through its high conductivity [25]. GO, which can be readily dispersed in water [19] and prepared in large quantities through the stripping of graphite under acidic and oxidizing conditions [26], possesses abundant carboxyl, hydroxyl, and epoxy groups on its base surface. Additionally, it exhibits a nanoscale domain comprising crystalline carbon or highly oxidized regions, allowing for the differential adsorption of biomolecules with varying affinities in different regions. Upon the successful preparation of the GO interface, fluorescence-based determination represents a commonly employed method for target detection. This method relies on the interference of external substances with the interaction between dye-labeled biomolecules and GO [27]. Iwe et al. [28] introduced a fluorescence-based method for DNA determination, utilizing GO, exonuclease III (Exo III), and specially designed fluorophore-labeled hairpin probes (HP1 and HP2). This approach capitalizes on the differential binding ability of GO towards hairpin DNA probes and single nucleotides (Figure 1a). Based on this principle of binding difference, many GO-based biosensor interfaces have been constructed for the detection of DNA or DNA-related biomolecules [29–31]. Affected by DNA hybridization [32], changes in voltage, current, or impedance may accompany DNA hybridization in GO-structured biosensor interfaces. Zhao et al. [6] synthesized a controllable flower-like Pt–graphene oxide (PtNFS-GO) structure via the layer-by-layer electrostatic self-assembly method and used it for biosensing research on DNA damage marker 8-hydroxy-2′-deoxyguanosine (8-OHdG). The PtNFS-GO structure, which resulted from the improved combination facilitated via electrostatic self-assembly, demonstrated high conductivity and exhibited an excellent electrochemical biosensor performance for the oxidation state of 8-OHdG.

The reduction from GO to reduced graphene oxide (rGO) introduces a higher density of defects, resulting in enhanced electrochemical activity compared to GO. This property proves particularly advantageous for the development of electrochemical biosensors [33]. Furthermore, rGO inherits the unique morphological structure and characteristics suitable for sensing applications. Cao et al. [34] reported on the combination of rGO and exonuclease III, which enables signal amplification in electrochemical impedance spectroscopy for DNA detection. By employing enzyme-assisted target recycling, the biosensing system transitions from a high-impedance state, in which ssDNA probes are directly adsorbed onto rGO, to a low-impedance state generated by the continuous desorption of target-probe ssDNA hybrid products and ssDNA probe digestion (Figure 1b). This approach allows for efficient interfacial tuning, and the change in the electron-transfer resistance becomes more pronounced after the removal of the ssDNA probe. As a result, changes in impedance signals can be measured to sensitively detect ssDNA targets with a remarkably low detection limit (LOD) of 10 aM. In recent practical applications, Ali et al. [35] reported an advanced biosensing platform based on rGO nanomaterials capable of the rapid detection of COVID-19 antibodies. They employed rGO nanosheets, immobilized specific viral antigens on their surfaces, and integrated the electrode with a microfluidic device. When antibodies were introduced to the electrode surface, they selectively bound to the antigens, and the binding event was detected by monitoring the impedance spectrum.

The examples above show that graphene nanomaterials and their derivatives play important roles in biosensor interfaces.

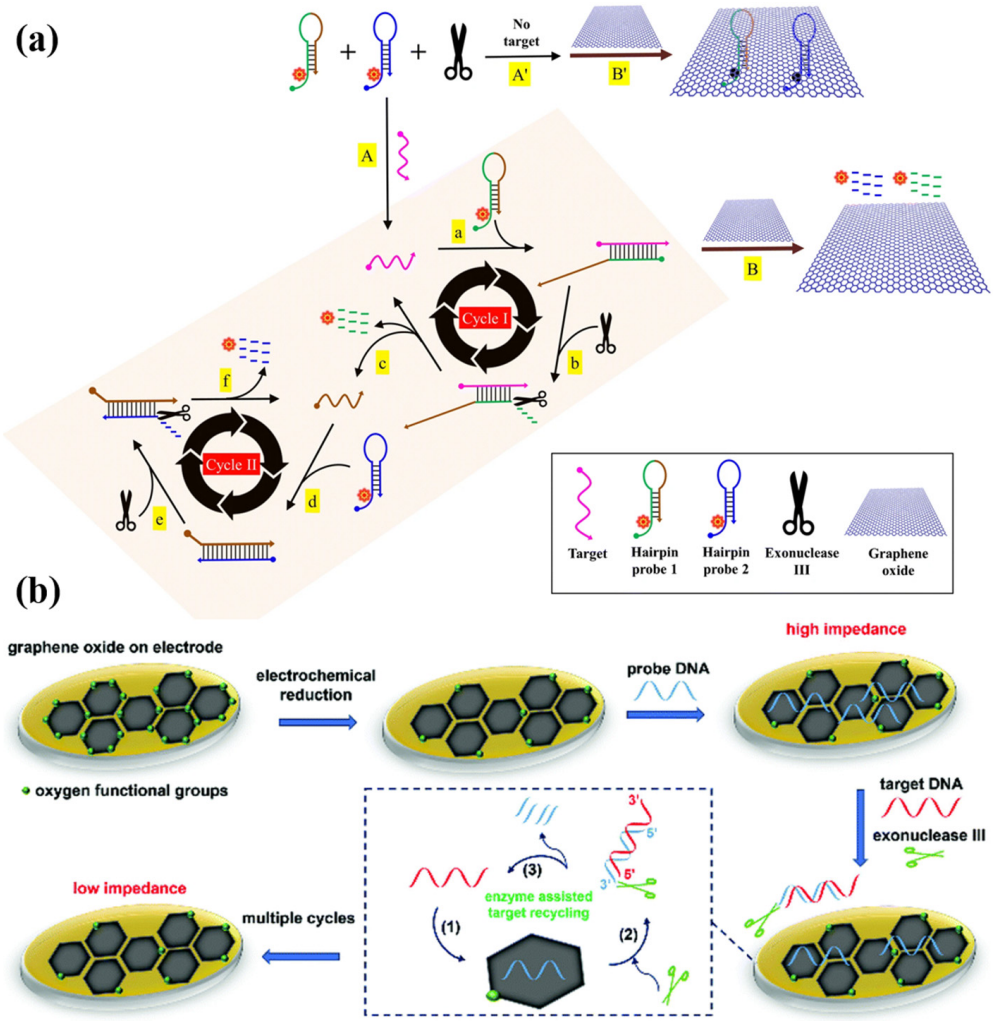

Figure 1. (**a**) Schematic of the detection strategy. On addition of GO without the presence of the target DNA (path A′), HP1 and HP2 are adsorbed onto the GO surface, giving rise to a low background signal (path B′). Upon the addition of the target DNA (path A), it hybridizes and forms a duplex structure with HP1 (a). The HP1-target DNA complex in cycle I allows Exo III to digest HP1 from the 3′ blunt end (b) to free the part of HP1 complementary to HP2, release the fluorophore, and regenerate the target DNA (c). In cycle II, the released fragment of HP1 binds with HP2 (d) and activates the enzyme again (e) to digest HP2, free the fluorophore, and release a fragment of HP1 to repeat the cycle (f). The subsequent addition of GO (path B) cannot quench the fluorescence of FAM, leading to the production of a strong fluorescence signal Reprinted with permission from [28], copyright 2019, *Microchimica Acta*. (**b**) Schematic representation of the fabrication of DNA impedimetric biosensor and its detection through enzyme-assisted target recycling. After the target DNA binds to the probe DNA on the electrode (path 1), exonuclease III is added to selectively hydrolyze the DNA probe in the double-stranded structure (path 2), and the released target DNA will bind to another probe to initiate another round of exonuclease III digestion (path 3). Reprinted with permission from [34], copyright 2019, *Analyst*.

Porous Carbon

Porous carbon possesses notable advantages, including a high specific surface area and superior electron-transfer performance, making it a promising candidate for biosensor applications [36]. In recent years, there has been significant interest in porous carbon derived from biomaterials due to its ease of preparation through low-cost precursor carbonization. Guan et al. [37] prepared a self-powered biosensor using lactate oxidase-modified porous-carbon film. This porous-carbon film exhibits the ability to absorb sweat and generate

electricity by harnessing the heat from natural sweat evaporation. The output voltage of the biosensor increases in proportion to the concentration of lactic acid present in sweat. Furthermore, the surface enzymatic reaction alters the zeta potential of the carbon, thereby influencing the output voltage. Gao et al. [38] utilized a luminescent reagent, luminol, for the in situ reduction in chloroauric acid on the nanopores of porous carbon. By combining this approach with an enzyme-cycle and chain-replacement mechanism, they achieved the ultra-sensitive detection of mucin1, an important tumor biomarker. The incorporation of Au-Lum nanoparticles (NPs) within the pores and hollow interiors of porous-carbon-accelerated electron transfer, resulting in excellent luminescence properties of the composite (Figure 2a). Tian et al. [39] designed an accurate biosensor based on n-doped porous-carbon-containing Fe (Fe/N-C) nanocomposites for the detection of H_2O_2 in real water samples and renal epithelial 293T cells. The Fe/N-C nanocomposites substantially enhanced the electron-transfer process and catalytic activity of the sensor, enabling the detection of trace amounts of H_2O_2. This development holds significance for various applications, such as monitoring H_2O_2 levels in water samples and studying its impact on renal epithelial cells.

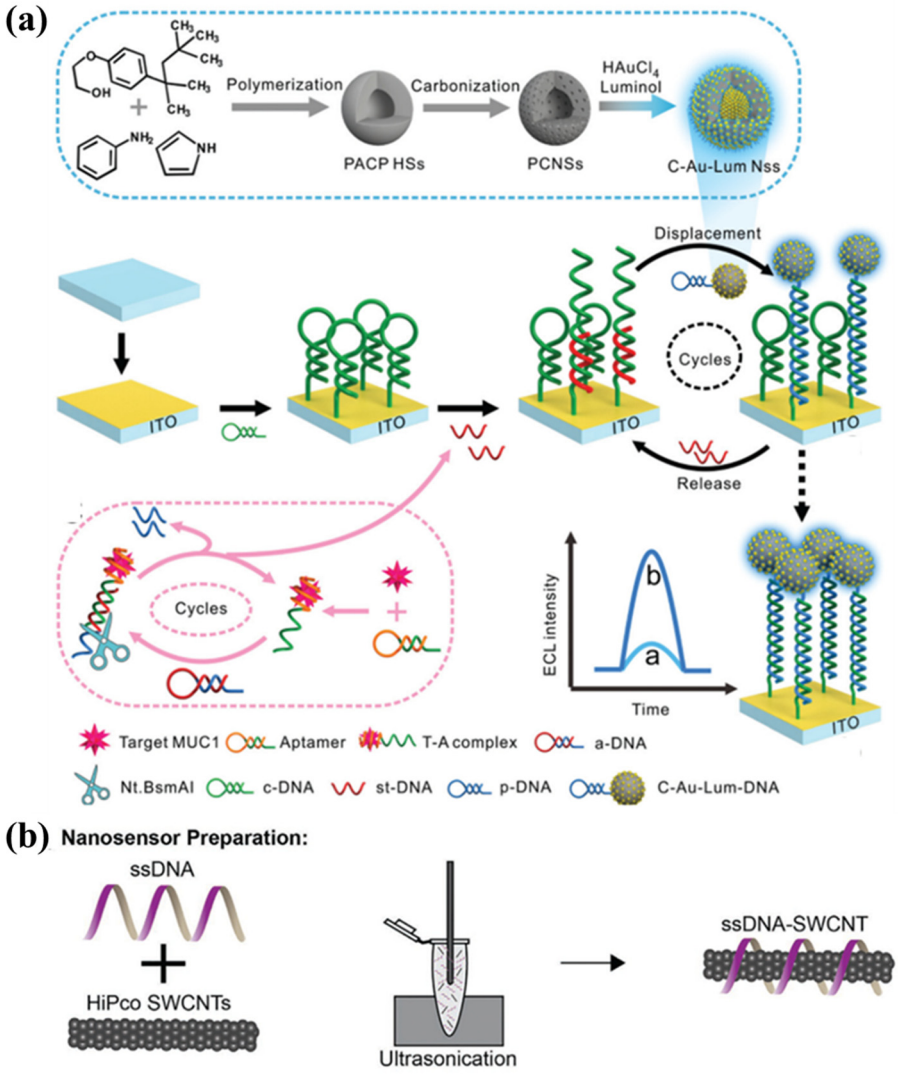

Figure 2. (**a**) The schematic of ECL biosensors for MUC1 detection. After further integrating with proximity-initiated secondary target DNA strand displacement (**a**), the ECL signal quality was significantly higher than that before replacement (**b**). Reprinted with permission from [38], copyright 2019, *Nanoscale*. (**b**) Nanosensor preparation via probe-tip sonicating SWCNTs in the presence of ssDNA followed by ultracentrifugation of the resultant dispersion. Reprinted with permission from [40], copyright 2021, *Advanced Functional Materials*.

Carbon Nanotubes

Carbon nanotubes, resembling rolled-up graphene cylinders, exhibit remarkable tensile strength, high conductivity, and excellent electrocatalytic abilities [41]. Single-walled carbon nanotubes (SWCNTs) consist of a single graphene cylinder, while multi-walled carbon nanotubes (MWCNTs) are composed of multiple layers [42,43]. Notably, through a comprehensive analysis of the existing literature, Gooding et al. [44] observed that SWCNTs outperformed their MWCNT counterparts in terms of electroanalytical performance. Although SWCNT-based electrodes expose a larger number of surface oxides to reactants and facilitate faster electron transfer, the reaction primarily occurs in a non-oriented manner, with the sidewalls predominantly immersed in the solution. This arrangement hampers the transmission and detection of the charge [36]. Consequently, current research predominantly focuses on SWCNTs. Exploiting the excellent light stability and fluorescence properties of SWCNTs in the near-infrared (NIR) range, which lies outside the autofluorescence region of chlorophyll, Lew et al. [45] developed a detection platform utilizing a pair of DNA-coated SWCNT probes. This ratio measurement platform enabled the in vivo detection of endogenous hydrogen peroxide in plants. The functionalized biosensing interface not only holds potential for monitoring H_2O_2 levels in human tumors, but also finds application in monitoring the therapeutic response of pancreatic ductal adenocarcinoma (PDAC) cells to tumors in vitro and in vivo, as well as in evaluating the efficacy of chemotherapy drugs (Figure 2b), as demonstrated by Bhattacharya et al. [46]. Safaee et al. [40] employed optical core–shell microfiber textiles incorporating SWCNTs for the real-time optical monitoring of the hydrogen peroxide concentration in in vitro wounds, enabling the tracking of the wound-healing progress. The versatility of the SWCNT biosensor extends to other applications depending on the utilization of wrapped single-stranded DNA. For instance, Harvey et al. [47] selected this implantable optical biosensor to swiftly quantify the exposure of doxorubicin in living tissues. Furthermore, Salem et al. [48] devised a sensor capable of distinguishing Cu(II), Cd(II), Hg(II), and Pb(II) at a concentration of 100 μM.

2.1.2. Polymer and Bio-Nanomaterials

Conducting polymers possessing favorable electrochemical properties, nanostructural morphology, and biological-coupling functionality play a crucial role in polymer biosensor systems. To reduce reliance on traditional nanomaterials, Meng et al. [49] employed tetrabutylammonium perchlorate as a soft template to fabricate a bifunctional poly(3,4-ethylenedioxythiophene) (PEDOT) interface with an adjustable 3D nanofiber network and carboxylic acid groups. This was achieved by controlling the copolymerization of 3,4-ethylenedioxythiophene(EDOT) and EDOT-COOH monomers (Figure 3a). The newly developed Bio-Nano-PEDOT-COOH interface allows for the coupling of various biorecognition molecules through the carboxylic acid groups, enabling the development of advanced all-polymer biosensors. Expanding on this work, Zhao et al. [50] demonstrated the sensitive and specific monitoring of 17β-estradiol (E2) by modifying electrodeposited PEDOT-graphene oxide (GO) with Au@Pt nanocrystals (Au@Pt). The PEDOT-GO nanocomposite film was polymerized in situ on a glassy carbon electrode using cyclic voltammetry, followed by the synthesis of Au@Pt on the conductive polymer. This provided a platform for aptamer immobilization. With the addition of E2, the differential pulse voltammetry signal gradually decreased due to hindered electron transfer at the E2–aptamer complex interface. Additionally, Zhu et al. [51] investigated the self-assembly of size-controlled tetrahedral framework nucleic acids (FNAs) on a microfluidic microchannel interface, allowing the elevation of DNA probes from the interface to construct a nanoscale three-dimensional reaction space. The highly ordered orientation, configuration, and density of the DNA probes within this three-dimensional reaction space optimize the reaction kinetics in molecular recognition processes. The FNA-designed interface was successfully applied to the one-stop detection of Escherichia coli O157:H7 (*E. coli* O157:H7), achieving a bacterial detection efficiency of 10 CFU/mL with excellent selectivity and precision. In

recent advancements, the design and development of polymer-based biosensing platforms for detection have been realized through novel analytical and scientific methodologies.

2.1.3. Other Nanomaterials

Besides the graphene nanomaterials and polymer and bio-nanomaterials mentioned earlier, various other nanomaterials, such as metal nanomaterials and metal oxide nanomaterials, have also been explored [52,53]. Zhou et al. [54] introduced a novel class of chameleon DNA-template silver nanoclusters (AgNCs) capable of switching fluorescence colors among red, orange, and yellow in response to Mg^{2+}, non-fluorescent auxiliary AgNC and complementary DNA. Based on this principle, a ratiometric fluorescence analysis platform was developed for the detection of target DNA. The yellow fluorescence of the probe increased, and the red fluorescence weakened as the amount of target DNA decreased. Regarding metal oxide nanomaterials, Fan et al. [55] discovered that MnO_2 nanosheets (NSs) can effectively quench the fluorescence of highly fluorescent Scopoletin (SC) while enhancing the fluorescence of non-fluorescent Amplex Red (AR) through an oxidation reaction. Upon the addition of glutathione (GSH), MnO_2 was reduced to Mn^{2+} and lost the oxide properties (Figure 3b). At this stage, the fluorescence of the SC intensified, and the AR was quenched. The biosensor system monitors GSH levels by detecting changes in the fluorescence signals of SC and AR.

Another commonly employed nanomaterial is MoS_2, a layered 2D transition metal dihalide exhibiting unique structural, physicochemical, optical, and biological properties [56]. Yan et al. [57] developed an aptasensor using hierarchical MoS_2 nanostructuring and SiO_2 nano-signal amplification. In this approach, hierarchical MoS_2 nanostructures served as functional interfaces, enhancing the accessibility between molecules and improving the efficiency of DNA hybridization. Simultaneously, the SiO_2 nanoprobes, combined with electroactive labels and DNA probes, amplified the electrochemical signal. This biosensing system enabled the simultaneous detection of prostate-specific antigen (PSA) and sarcosine, two prostate cancer (PCa) biomarkers.

Overall, nanomaterials play a pivotal role in the functionalization strategies of biosensing interfaces. Table 1 provides a comparison of nanostructure-functionalized biosensor interfaces.

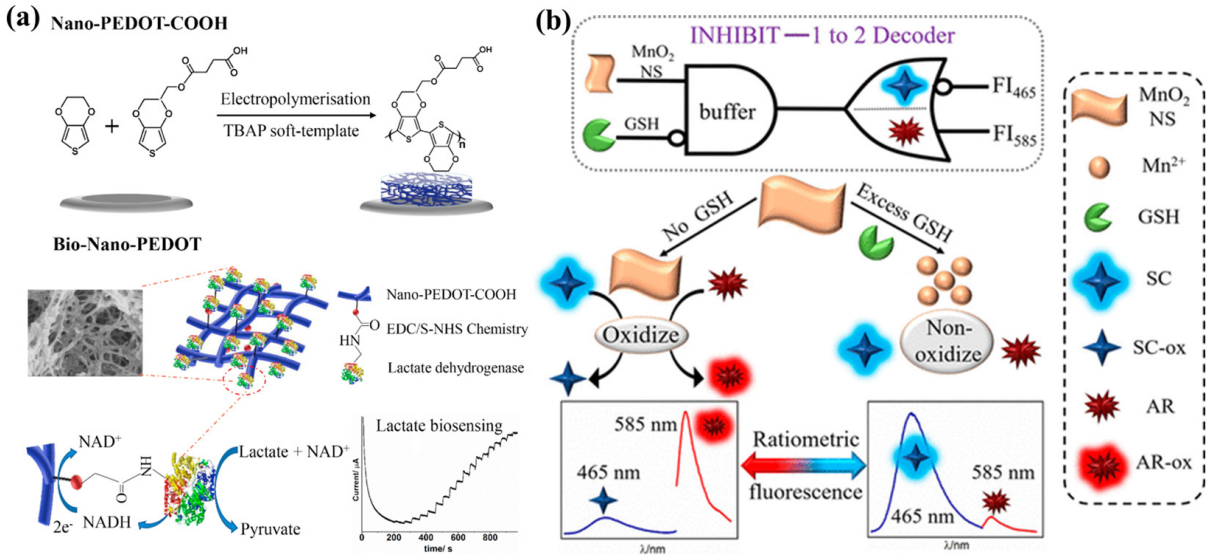

Figure 3. (**a**) Schematic of 3D Nano-PEDOT-COOH network preparation via copolymerization of EDOT and EDOT-COOH monomers using TBAP as a soft template; Bio-Nano-PEDOT; Nano-PEDOT-COOH bio-conjugation with lactate dehydrogenase via EDC/S–NHS chemistry for lactate biosensing. Reprinted with permission from [49], copyright 2022, *Biosensors and Bioelectronics*. (**b**) Schematic operations of the MnO_2 NS-based ratiometric fluorescent sensor for GSH based on two fluorescent substrates. Reprinted with permission from [55], copyright 2017, *ACS Appl Mater Interfaces*.

Table 1. Comparison of nanostructure-functionalized biosensor interfaces.

Functionalized Goal	Functionalized Strategy	Nanostructure	Principle	Effect	Reference
Fluorescence analysis detection of hemochromatosis protein gene	Direct adsorption	GO	π-stacking interactions	Ensures a very low background signal	[28]
Specific detection of biomarker-8-hydroxy-2′-deoxyguanosine	Layer–layer electrostatic self-assembly	GO	Electrostatic interaction	Improves the electrocatalytic performance of Pt nanoparticles	[6]
Detection of ultrasensitive target DNA	Direct adsorption	rGO	π-stacking interactions	Enlarges impedimetric signals	[34]
Detection of COVID-19 antibodies within seconds	Amidation reaction	rGO	Covalent bond	Enhances the transport of diffusing species in an electrochemical cell	[35]
Building of a self-powered wearable-lactate analyzer	Direct adsorption	Porous carbon	π-stacking interactions	Soaks up environmental thermal energy to generate electricity	[37]
Achievement of an ultrasensitive ECL biosensor	In situ reduction	Porous carbon	Electron transfer	Increases the mass transfer of reagents; accelerates the electron transport	[38]
Development of a highly sensitive and selective ECL * sensor based on the noble metal-free electrode	Pyrolytic process	Porous carbon	Breaking and polymerization of molecular bonds	Facilitates rapid electron transfer; improves the conductivity of the electrode	[39]
Real-time, in situ biochemical measurement of H_2O_2 in plants	DNA wrapping	SWNT	π-stacking interactions	An ideal probe for in vivo plant applications	[45]
Detection of H_2O_2 to determine the response to tumor therapy	DNA wrapping	SWNT	π-stacking interactions	Determines dynamic alteration of hydrogen peroxide in tumor; evaluates the effectiveness of chemotherapeutics	[46]
Continuous monitoring of ROS through a wearable diagnostic platform to prevent chronic and pathogenic infections	DNA wrapping	SWNT	π-stacking interactions	In situ measurements of peroxide in wounds	[40]
Use of implantable optical nanosensors to rapidly quantificate doxorubicin in living tissues	DNA wrapping	SWNT	π-stacking interactions	Quantifies doxorubicin exposure to tissues within living organisms	[47]
Fixing of near-infrared fluorescent SWCNT sensor on the paper substrate for sensing	DNA wrapping	SWNT	π-stacking interactions	Immobilizates SWCNTs onto paper substrates; distinguishes metal-ion contaminants	[48]

Table 1. *Cont.*

Functionalized Goal	Functionalized Strategy	Nanostructure	Principle	Effect	Reference
Fabrication of a Bio-Nano-PEDOT *-based biosensor for lactate detection	EDC/S–NHS chemistry	PEDOT-COOH	Chemical coupling	Low charge-transfer resistance; high transduction activity towards the co-enzyme NADH	[49]
Preparation of an electrochemical aptasensor electrodeposited of PEDOT *-GO coupled with Au@Pt	EDC/S–NHS chemistry	PEDOT-COOH	Chemical coupling	Fabricates a simple, label-free electrochemical aptasensor to detect estradiol	[50]
Development of an integrated "one-stop" microfluidic biosensor	Complementary base pairing	Framework nucleic acids	Hydrogen bond	One-stop detection of E.Coli O157:H7 with capture, release, enrichment, cell culture, and antimicrobial susceptibility testing	[51]
Detection of dual PCa * biomarkers, PSA and sarcosine	DNA wrapping	DNA-SiO_2	π-stacking interactions	Enhances the diagnostic performance of PCa *	[57]

* ECL: electrochemiluminescence; PEDOT: poly (3,4-ethylenedioxythiophene); PCa: prostate cancer.

2.2. Small-Molecule-Mediated Interfacial Regulation

Small molecules offer several advantages, including good biocompatibility, clear structures, and easy modification, making them versatile for biosensor functionalization [58]. For instance, Cui et al. [59] utilized dopamine as a functional monomer to synthesize graphdiyne (GDY) with high biocompatibility and conductivity through hydrogen bonding and multipoint electrostatic attraction. They incorporated GDY into C-reactive molecular-imprinted polymers (C-MIPs), achieving high sensitivity and selective recognition of human C-reactive protein (Figure 4a). Salimian et al. [60] employed polyethylene glycol to modify the sensing interface, effectively preventing non-specific protein adsorption and enabling the sensitive and specific detection of cancer biomarkers in serum. Similarly, Zhang et al. [61] employed 6-mercapto-1-hexanol to modify DNA probes and immobilized them on the gold-nanoparticle interface to analyze DNA methylation through current changes.

Fluorescent probes based on small molecules have also found widespread application in the detection of crucial biological analyses [62]. These probes undergo changes in luminescence intensity or emission wavelength through various sensing mechanisms. Among them, electrochemiluminescence (ECL), also known as electrogenerated chemiluminescence, stands out as a superior method for biosensing compared to other photoexcitation spectroscopy techniques. ECL involves the generation of free radicals on the electrode surface, which undergo high-energy electron-transfer reactions to form excited states and emit light [63]. Consequently, ECL does not require excitation light and exhibits minimal background signals [64]. Currently, luminol serves as the most commonly used organic-small-molecule ECL emitter. Zhao et al. [65] developed a paper-based dual-mode detection platform to detect Pb^{2+} based on the oxidation reaction initiated by horseradish peroxidase (HRP) in the presence of H_2O_2. Upon the addition of Pb^{2+} to the interface, cleaved oligonucleotide fragments linked to HRP-functionalized Au nanocubes penetrated into the cellulose, quenching the ECL signals of CDs and quantum dots via resonance energy transfer [63] while enhancing the ECL intensity generated by luminol catalyzed by H_2O_2 (Figure 4b). On this basis, Guo et al. [66] further advanced the field by using reactive oxygen species (ROS) instead of H_2O_2 to develop a new luminol-ROS ECL system for GSH

detection. The dissolved oxygen was reduced to superoxide radicals (O_2^-) by atomized gold-loaded 2D VO_2 nanobelts (Au/VO_2), which combined with the loaded luminol to promote the ECL. The ECL resonance energy transfer (ECL-RET) between the hollow SiO_2 nanospheres and luminol resulted in a significant decrease in the ECL-signal response. In the presence of GSH, the effective redox reaction between SiO_2 and GSH restored the ECL signal.

Due to distinct luminescence mechanisms and low electroluminescence efficiency in the aqueous phase, most small organic molecules are unsuitable for recognition and response analysis, limiting their application in biosensing [67]. Therefore, further research is needed to explore the interfacial regulation mediated by organic electroluminescent small molecules. Table 2 shows a comparison of small-molecule-functionalized biosensor interfaces.

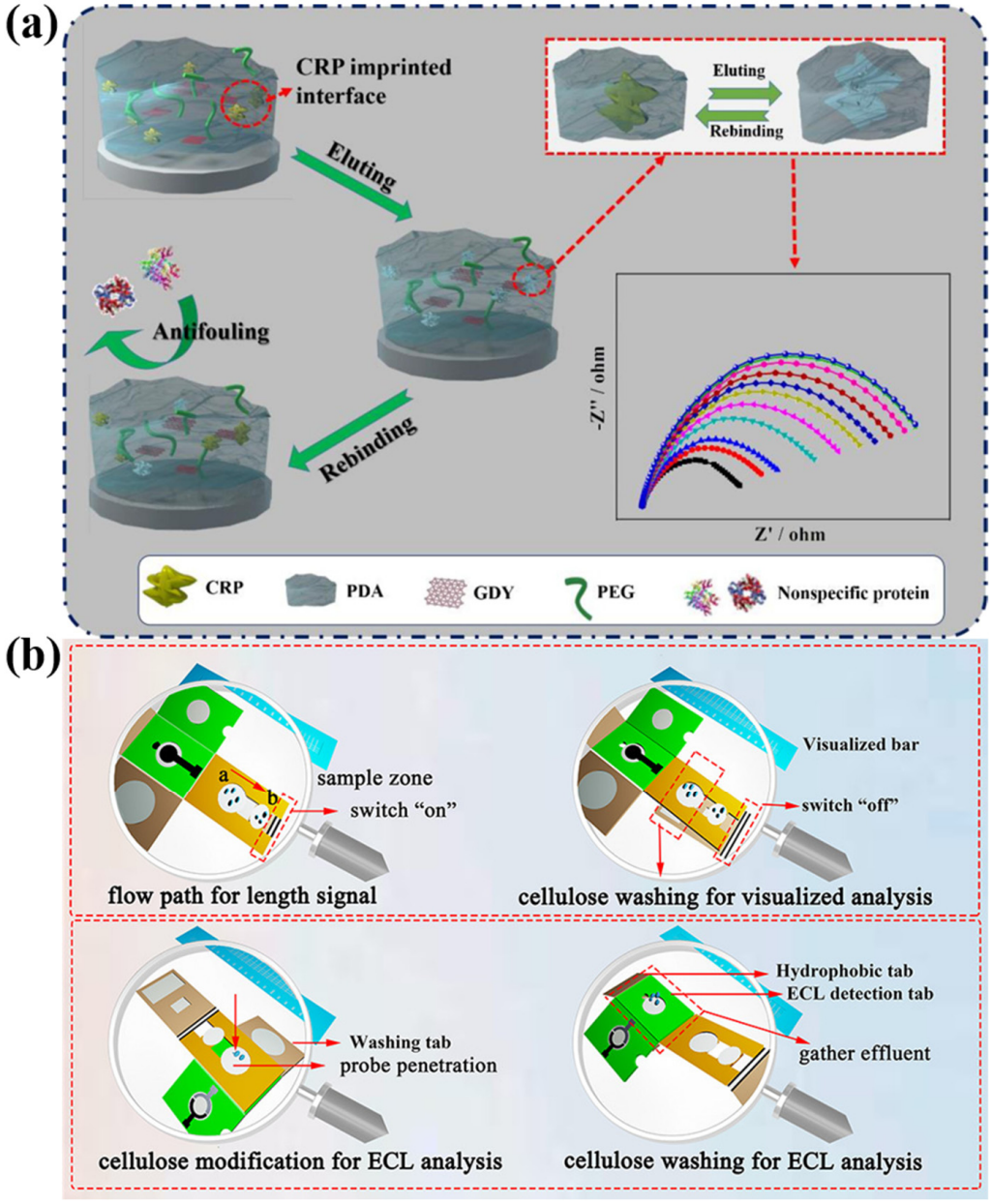

Figure 4. (**a**) Schematic process of the GDY-based CRP-imprinted biosensor. Reprinted with permission from [59], copyright 2022, *Chemical Engineering Journal*. (**b**) Illustration of assembly and operating process of the dual-mode lab-on-paper device. Reprinted with permission from [65], copyright 2020, *Anal. Chem*.

Table 2. Comparison of small-molecule-functionalized biosensor interfaces.

Functionalized Goal	Functionalized Strategy	Small Molecule	Principle	Effect	Reference
Construction of a highly sensitive protein MIP biosensor	MIT *	Dopamine	Hydrogen bond, multipoint electrostatic attraction	Achieves the highly sensitive and selective recognition of human C-reactive protein	[59]
Development of an electrocatalytically amplified assay for analysis of HER-2 *	Reaction of Au with mercapto groups	Polyethylene glycol	Au-S bond	Achieves sensitive and specific sensing of cancer biomarkers in serum	[60]
Preparation of an electrochemical sensor via the co-assembling of DNA probe and 6-mercapto-1-hexanol onto a gold electrode	Reaction of Au with mercapto groups	6-mercapto-1-hexanol	Au-S bond	Analyzes dynamic DNA methylation process	[61]
Integration of visual readings and ratiometric ECL analysis on paper substrates	Direct adsorption	Luminol	Au-N bond, electrostatic interaction	Obtains accurate monitoring performance for H_2O_2	[65]
Preparation of a new luminol-ROS ECL system to detect GSH *	Direct adsorption	Luminol	Au-N bond, electrostatic interaction	Greatly promotes the ECL emission	[66]
Forster resonance energy transfer based ratiometric imaging of lysosomal HOCl *	Redox reaction	Non-fluorescent spirothioether unit	Electron transfer	Exhibits distinct biochemical properties for facile monitoring of HOCl via conventional flow cytometry	[68]
Exhibition of high detection sensitivity to $OONO^-$ *	Chemical reaction	Cyanine 3, cyanine 5	Condensation reaction	Produces a ratiometric fluorescence signal	[69]
Development of "smart" noninvasive bioimaging probes for trapping specific enzyme activities	Substitution reaction	β-galactosidase	Nucleophilic substitution	Real-time fluorescence quantification; capture of in vivo and in situ β-GAL activity	[70]
Use of new fluorophore (azulene) to prepare an effective two-photon fluorescent probe	Inversion of internal charge transfer	Boronate	Electron transfer	Detects reactive oxygen species; has good cell penetration	[71]
Development of fluorescent probes that can show different modes of fluorescence signals fo distinct concentrations	Substitution reaction	2,4-dinitrobenzenesulfonate, the chloro group	Nucleophilic substitution	Shows the signal in the low-concentration range of thiols and the ratio response to high-concentration thiols	[72]
A conformationally induced "off–on" tyrosine kinase cell membrane fluorescent sensor	Linker group connectivity	Sunitinib, pyrene	Hydrogen bond	Enables fluorescence microscopy imaging of receptor protein tyrosine kinases in the cell membranes of living cells	[73]

Table 2. *Cont.*

Functionalized Goal	Functionalized Strategy	Small Molecule	Principle	Effect	Reference
Design of a mitochondria-specific coumarin pyrrolidinium-derived fluorescence probe	Linker group connectivity	7-diethylamino-coumarin moiety	Hydrogen bond	Allows real-time ratio imaging of HCN in living cells	[74]

* MIT: molecular-imprinting technology; HER-2: human epidermal growth factor receptor-2; GSH: glutathione; HOCl: hypochlorous acid; $OONO^-$: peroxynitrite.

2.3. Biomacromolecule-Mediated Interfacial Regulation

In response to the growing demand for biosensing, the development of biomacromolecule-mediated sensing interfaces with precise molecular recognition, controllable signal amplification, and enhanced sensing performance has become imperative. Various biomacromolecules, including enzymes, DNA, proteins, and cells, have been employed to modify the sensing interface, enabling the creation of highly sensitive and selective biosensors [32].

2.3.1. Enzyme-Based Interfaces

Enzymes, in particular, are widely utilized components in biosensor interfaces, leveraging their ability to detect targets with high specificity through the catalytic conversion of the analyte or enzyme inhibition [7]. To achieve a superior sensing performance, it is crucial to immobilize efficient biological enzymes onto the sensing interface while preserving their biological properties. Consequently, numerous immobilization methods have been developed, ranging from membrane encapsulation and physical adsorption to covalent binding [75].

For example, Gu et al. [76] employed a membrane encapsulation method to modify the electrode surface with glucose oxidase (GOx) for glucose sensing (Figure 5a). They utilized a 3D porous $Ti_3C_2T_x$·Mxene–graphene (MG) hybrid film with an adjustable porous structure, which provided a highly hydrophilic microenvironment for GOx immobilization. Dhanjai et al. [77] employed chitosan (CHI) as a binder for the physical adsorption of glucose oxidase (GOx) onto a cobalt oxide-loaded mesoporous carbon framework (Co_3O_4 @ MCF), enabling highly selective glucose detection upon the modification of a glassy carbon electrode. Levien et al. [7] covalently linked GO_x and acetylcholinesterase (AChE) onto the surface of plasma-polymerized (pp) hydrogels to fabricate an electrochemical biosensor interface. They utilized glucose as the substrate for GOx and eserine as the AChE inhibitor to validate the practicality of the biosensing approach.

2.3.2. DNA-Based Interfaces

DNA, a genetic biological macromolecule, plays a crucial role in regulating life activities with remarkable accuracy. Additionally, DNA possesses the unique attribute of sequence programmability, allowing for the incorporation of desired functions through well-designed sequences [78]. Currently, DNA modifications can be broadly categorized into chain DNA, DNA nanomaterials, and framework DNA (FDNA) [79–81]. For instance, Su et al. [80] investigated the impact of probe DNA on the detection performance of adenosine triphosphate aptamer (ATPA) and adenosine triphosphate (ATP) in the presence of hairpin DNA and double-stranded DNA (DsDNA). Subsequently, Zhu et al. [82] separated the two and developed two aptamer sensors based on hairpin DNA (HDNA) and linear single-stranded DNA (ssDNA) for the detection of aflatoxin B1 and diethyl phthalate.

In the DNA/nano-functionalized electrochemical sensing interface, thiol-modified DNA is immobilized on the gold-electrode surface through strong gold–thiol interactions [81]. Miao et al. [83] proposed an electrochemical biosensor utilizing DNA-modified Fe_3O_4 @ Au magnetic NPs (Figure 5b). The three DNA probes contain specific

mismatched base pairs, and the presence of different heavy-metal ions promotes hybridization with distinct DNA probes, enabling the detection of corresponding electrochemical species on the magnetic nanoparticle surface. Han et al. [84] anchored methylene blue-labeled polyadenine DNA onto a gold electrode to construct an electrochemical biosensor interface for the detection of the COVID-19 virus.

Comparatively, FDNA offers a higher probe density on the electrode surface compared to DNA nanomaterials [79]. Su et al. [85] covalently coupled DNA tetrahedrons to the carbon surface and applied them for the detection of various bioactive molecules. Furthermore, Mao et al. [86] developed a three-dimensional pure DNA hydrogel serving as a scaffold for electron transfer. The DNA hydrogel incorporates an embedded electron mediator through binding, while DNAzyme is introduced at the hydrogel scaffold nodes to enable the long-range acquisition of DNAzyme catalytic signals.

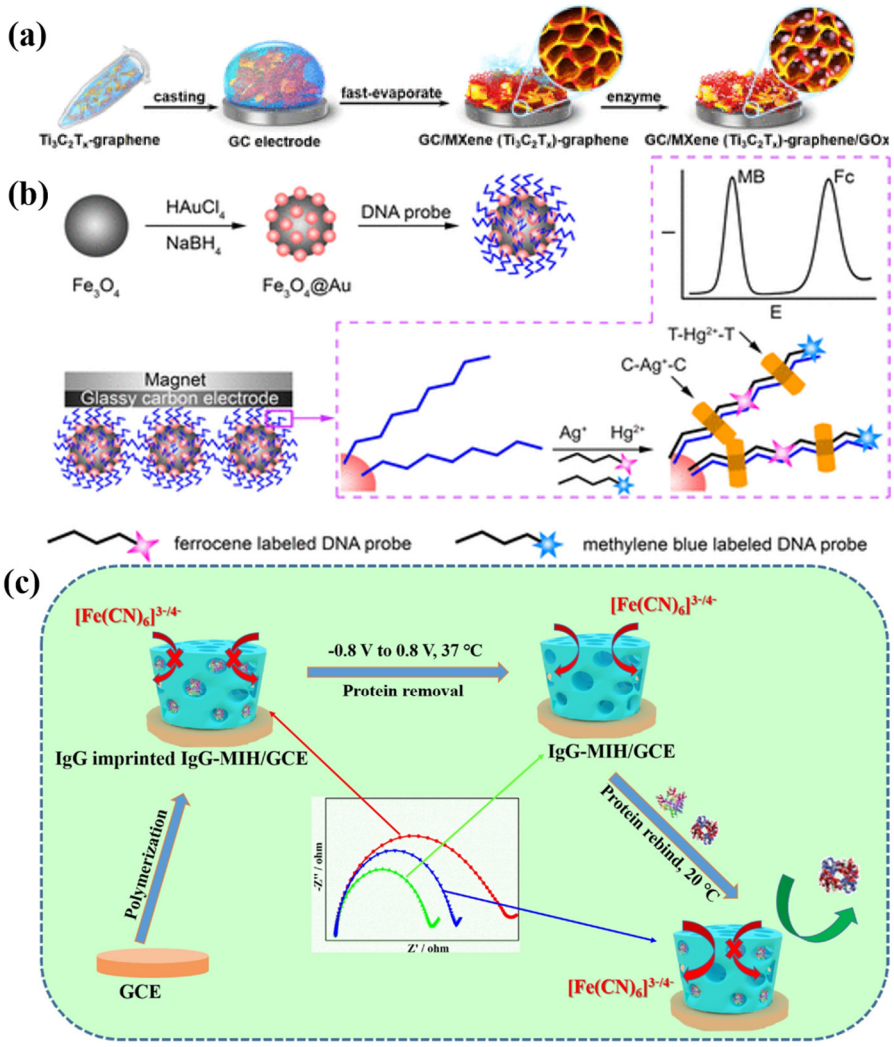

Figure 5. (**a**) Preparation of MG hybrid film for enzyme immobilization. Reprinted with permission from [76], copyright 2019, *ACS Applied Nano Materials*. (**b**) Preparation schematic diagram of DNA-modified Fe_3O_4@Au NPs and detection of Ag^+ and Hg^{2+}. Reprinted with permission from [83], copyright 2017, *ACS Appl Mater Interfaces*. (**c**) Schematic fabrication protocol of the electrochemical biosensor based on IgG-imprinted hydrogel. Reprinted with permission from [87], copyright 2021, *Sensors and Actuators B: Chemical*.

2.3.3. Protein-Based Interfaces

Proteins, as quintessential biological macromolecules, exhibit distinct binding affinities and sequence specificities towards DNA and RNA, as elucidated by Berezovski et al. [88].

For instance, Campuzano et al. [89] demonstrated that Tombusviral p19 protein forms dimers and selectively binds to short dsRNA, making it a valuable tool for identifying miRNAs upon hybridization with specific RNA probes. Rubio et al. [90] harnessed the concept of de novo-designed protein switches to create protein-based biosensors, enabling the reversal of information flow. Applying this approach, they developed a biosensor for the SARS-CoV-2 spike protein, incorporating a de novo-designed spike receptor-binding domain (RBD) binder4, with a remarkable limit of detection of 15 pM. Innovative techniques involving the combination of proteins and molecular-imprinting technology (MIT) have led to the development of protein-imprinted hydrogels (MIHs) [91]. Extensive efforts have been made in this area. Utilizing free-radical polymerization, a new type of protein-imprinting hydrogel was created by combining N,N′-methylenebis(acrylamide) cross-linkers, N,N′-dimethylaminoethyl methacrylate gas-sensitive monomers, and human serum albumin (HSA) as the template protein. This hydrogel exhibited unique self-recognition properties towards HSA protein [92]. Furthermore, Cui et al. [87] synthesized a protein-imprinted hydrogel using acrylamide as a functional monomer through free-radical polymerization. This hydrogel demonstrated high sensitivity and selectivity for detecting target immunoglobulins in complex biological samples (Figure 5c).

2.4. Cell-Based Interfaces

Cell-mediated biosensing interfaces have emerged as promising tools in biomedicine [93]. For example, Qi et al. [94] utilized marine-pathogen sulfate-reducing bacteria (SRB) to facilitate the synthesis of bio-imprinted membranes, leading to the formation of a biosensing interface. The electrochemical impedance method enabled the direct measurement of the bacterial concentration. Building upon this work, Jiang et al. [95] employed electropolymerization to create a Salmonella-imprinted membrane, resulting in the development of a biosensor interface capable of detecting Salmonella within a short span of 20 min. In addition to molecular-imprinting technology (MIT), red blood cell (RBC)-mediated biosensing interfaces have also witnessed significant advancements. Shete et al. [96] employed a reversible membrane-opening/resealing method to incorporate a designed nanosensor into RBCs, facilitating the detection of exchangeable Pb^{2+} concentrations over time and space. Furthermore, Chen et al. [97] immobilized gold-coated Fe_3O_4 core–shell nanocomposites on RBCs, enabling the use of RBCs as cell biosensors for detecting H_2O_2. As technology continues to progress, cell-mediated interface regulation strategies are becoming increasingly sophisticated. In 2018, Liu et al. [98] combined red cell membrane vesicles with near-infrared persistent luminescent nanophosphors (PLNPs) and employed mesoporous SiO_2 as a carrier to fabricate a biosensor interface for the in situ monitoring of tumor-growth inhibition. Although there are relatively fewer examples of cell-mediated biosensing interfaces compared to nanomaterials and other biomolecules, their development prospects remain highly promising. This is attributed to the superior biocompatibility of cells, which allows biosensors to play a crucial role in human medicine. Table 3 shows a comparison of biomacromolecule-functionalized biosensor interfaces.

Table 3. Comparison of biomacromolecule-functionalized biosensor interfaces.

Functionalized Goal	Functionalized Strategy	Biomacro-Molecule	Principle	Effect	Reference
Construction of a 3D porous $Ti_3C_2T_x$ MG * hybrid film for the determination of glucose in serum	Membrane encapsulation	GO_x	Wrapped	Enhances the stable fixation and retention of GO_x in the membrane	[76]
Preparation of advanced functional nanostructures based on Co_3O_4@MCF *	Physical adsorption	GO_x	Hydrogen bond	Highly selective detection of glucose	[77]

Table 3. *Cont.*

Functionalized Goal	Functionalized Strategy	Biomacro-Molecule	Principle	Effect	Reference
Study of the bio-interaction properties of PP hydrogel composed of HEMA * and DEAEMA * on SPE	Covalent binding	GO_x	Covalent bond	Optimizes the response of the sensor via different biomolecular ratios	[7]
Construction of a targeted induced hairpin-mediated biosensing interface	Reaction of Au with mercapto groups	Hairpin DNA	Au-S bond	Enhances the effect of probe DNA on the detection performance of ATPA * and ATP *	[80]
Development of a dual-ratiometric electrochemical apta-sensing strategy for the simultaneous detection of AFB1 * and OTA *	Complementary base pairing	ssDNA	Hydrogen bond	Greatly improves the assembly and recognition efficiency of the sensing interface	[82]
Development of an electrochemical biosensor based on DNA-modified Fe_3O_4 @ Au magnetic NPs for the detection of trace heavy-metal ions	Reaction of Au with mercapto groups	DNA	Au-S bond	Detects heavy-metal ions with no obvious interference at the same time; maintains the high sensitivity	[83]
Proposition of an electrochemical aptamer sensor based on CRISPR/CAS12a	Reaction of Au with mercapto groups	Polyadenine DNA	Au-S bond	Detects COVID-19 NPs * rapidly and is ultrasensitive	[84]
Preparation of an electrochemical biosensor by using a specific DNA skeleton-DNA tetrahedron	Covalent binding	DNA tetrahedron	Covalent bond	Detects a variety of bioactive molecules with high signal-to-noise ratio, sensitivity, and specificity.	[85]
Construction of an electrochemical biosensor by introducing DNAzyme with peroxidase-like activity into the junction of hydrogel	Embedding binding	DNAzyme	π–π conjugation, hydrophobic interaction	Overcomes the limitation of two-dimensional electrode, obtains long-distance catalytic signal of DNAzyme	[86]
Construction of a specific and long-acting antifouling biosensor interface based on protein-imprinted hydrogel	Complex	Template protein IgG *	Multiple-point electrostatic interaction, hydrogen bond	Detects target immunoglobulins in complex biological samples	[87]
Preparation of a new gas-sensitive-imprinted hydrogel via free-radical polymerization	Free-radical polymerization method	π bond is broken and start of poly-merization reaction	Human serum albumin (HSA)-template proteins	Shows unique self-recognition characteristics to HSA protein	[92]

* MG: Mxene–graphene; GO_x: glucose oxidase; MCF: mesoporous carbon framework; HEMA: hydroxyethyl methacrylate; DEAEMA: 2-(diethylamino)ethyl methacrylate; SPE: gold screen-printed electrodes; ATPA: adenosine triphosphate aptamer; ATP: adenosine triphosphate; AFB1: aflatoxin B1; OTA: ochratoxin A; NP: nucleocapsid protein; IgG: immunoglobulin G.

3. Electro-Click Chemistry for the Functionalization of Biosensor Interfaces

In 2001, Sharpless et al. [8] first proposed the concept of connecting small units with heteroatom connections (C-X-C) to generate matter. They hope to develop a set of powerful and selective "modules" that can work reliably in both large and small applications. The basis of this method is named "click chemistry". In simple terms, click chemistry is a selective assembly of two molecular building blocks under mild reaction conditions. It has the characteristics of high yield, harmless by-products, and easy separation via non-chromatographic methods [14].

For click chemistry, carbon–heteroatom-bond-formation reactions are the most common examples, including cycloadditions of unsaturated species, nucleophilic substitution chemistry, carbonyl chemistry of the "non-aldol" type, and additions to carbon–carbon multiple bonds [8]. Then, researchers from the same group reported that the reaction rate and regioselectivity can be improved by using Cu(I) to catalyze the Huisgen dipolar cycloaddition in 2002 [99]. A few years later, Sharpless et al. [100] and Rodionov et al. [101] further found that Cu(I)-catalyzed alkyne–azide cycloaddition (CuAAC) can effectively form 1-4-disubstituted 1,2,3-triazole bonds in water and organic solvents (Figure 6). Today, CuAAC has become the most representative cycloaddition reaction, compatible with a wide range of solvents, pH values, and temperatures [102]. Of course, there are also the thiol–ene reaction, Michael addition reaction, imine and oxime reaction, and Diels–Alder cycloaddition reaction [103]. Click chemistry is considered an effective strategy to immobilize biomolecules while maintaining their biological activities [104–106]. This review will take the CuAAC click reaction as an example to introduce the development in recent years.

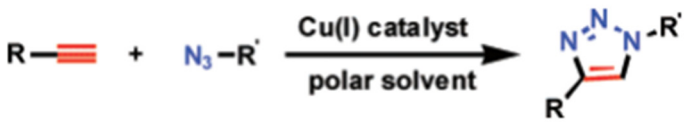

Figure 6. CuAAC process. Reprinted with permission from [107], copyright 2008, *J. Am. Chem. Soc.*

3.1. Traditional Click Technology

Because CuAAC is an addition reaction of azides and alkynes catalyzed by Cu(I), Cu(I) can be directly added to the reaction environment or in situ generated by the reaction of Cu(II) with reducing agents [9]. Although Cu(I) can be directly added to the reaction system, the development of stable Cu(I) catalysts is of great significance for the application of CuAAc due to the poor stability of Cu(I). Yang et al. [108] prepared $Cu_{2-x}S_ySe_{1-y}$ nanoparticles, which have a large number of Cu vacancies, and Cu(II) and Cu(I) coexist, to catalyze the click chemistry of CuAAC (Figure 7a). Because glutathione can stabilize Cu(I), Zhang et al. [104] successfully prepared a novel nanocatalyst containing abundant and stable Cu (I). Therefore, the reduction in Cu(II) by a reducing agent is also a common method of the CuAAC click reaction. Guerrero et al. [105] reported the first electrochemical immunosensor for the detection of CXCL7 (chemokine (C-X-C motif) ligand 7) as an autoimmune marker via the click reaction of azide-functionalized MWCNTs and ethynyl-IgG on screen-printed carbon electrodes using ascorbic acid to reduce the Cu(II) (Figure 7b). Then, Xue et al. [109] used specific antigen–antibody recognition to trigger the in situ reduction in Cu MOF, thereby generating a powerful click catalyst for the CuAAC click reaction.

However, as a catalyst, Cu(I) has certain toxicity, and some Cu-catalyzed fixed viruses or oligonucleotide chains will degrade [111]. Bertozzi et al. [112] first proposed copper-free click chemistry, which eliminates the adverse effects of Cu(I), simplifies the experimental steps, and becomes an alternative CuAAC click reaction. This is an alternative method to activate alkynes for the catalyst-free [3+2] cycloaddition reaction with azides. Then, Xiang et al. [110] reported a biosensor system based on azide-co-functionalized graphene oxide (GO-N_3) and carbon dots (CDs). Carbon-dot-labeled DNA (CD-DNA) binds to GO-N_3 by copper-free click chemistry and quenches the fluorescence of CDs by fluorescence

resonance energy transfer (FRET) (Figure 7c). After adding carcinoembryonic antigen (CEA), CEA binds to the aptamer and fluorescence recovers. The latest research progress was proposed by Yang et al. [113]. They designed and constructed a nanopore complex containing unnatural amino acid, which is a conical rigid complex formed by octameric Mycobacterium smegmatis porin A (MspA). Through the strain-promoted azide–alkyne cycloaddition reaction, single-stranded DNA composed of 40 thymines (poly-T(40)) and lysozyme molecules with dibenzocyclooctyne (DBCO) were successfully connected to the functionalized nanopore interface, and it was found that it exhibited a new signal distribution pattern and the signal was significantly enhanced. When combined with different oligosaccharide substrates, the corresponding signals will change significantly. The prepared functionalized interface provides a new direction for single-molecule sensing. We can see that click chemistry is also an attractive technique in the biomedical field. However, there are only a few papers on the latest application of click chemistry in the biomedical field [15].

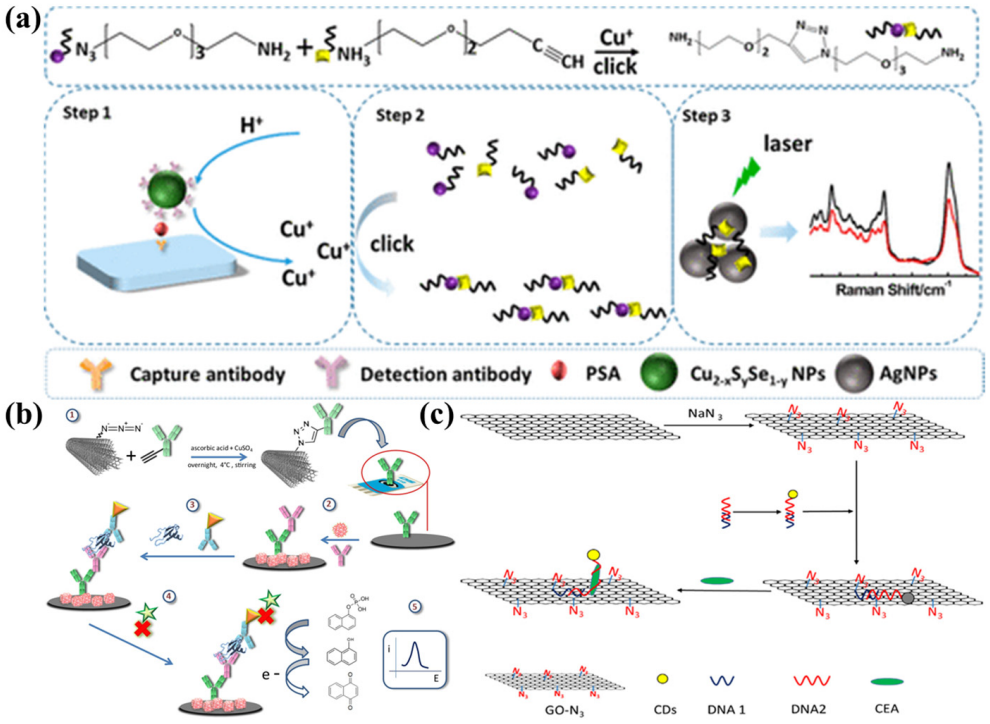

Figure 7. (**a**) $Cu_{2-x}S_ySe_{1-y}$-NP-catalyzed click chemistry for SERS immunoassay of PSA detection. Reprinted with permission from [108], copyright 2018, *Anal Chem*. (**b**) Schematic display of the different steps involved in the preparation of the immunosensor for the determination of CXCL7. Reprinted with permission from [105], copyright 2019, *Journal of Electroanalytical Chemistry*. (**c**) Schematic illustration of CEA detection system based on click chemistry and FRET between GO-N_3 and CD -DNA. Reprinted with permission from [110], copyright 2020, *Anal Chim Acta*.

3.2. Electro-Click Technology

In the CuAAC click reaction, Cu(I) salts or the in situ reduction in Cu(II) are commonly employed to introduce a catalytic amount of Cu(I). Various methods can be used to generate the required Cu(I) ions, including microwave [114], ultrasound [115], UV irradiation [116], and electrochemical reactions [117]. The electrochemical approach enables the reagent-free functionalization of biosensing interfaces, known as electro-click [16]. Devaraj et al. [118] demonstrated that catalytic Cu(I) ions can be generated by applying a mild reduction potential (−300 mV vs. Ag/AgCls) at the interface in contact with the Cu(II) solution. For example, Lesniewski et al. [119] deposited gold nanoparticles modified with terminal alkynyl groups onto azide-functionalized glassy carbon surfaces. The generation of the Cu catalyst can be precisely controlled by adjusting the treatment time, allowing

control over the surface coverage by altering the deposition time. Villalba et al. [120] achieved the catalytic assembly of multilayers through the covalent bonding of poly(acrylic acid) (PAA) multilayers with alkynyl (PAAalk) and azide (PAAaz) groups. Recently, Yamamoto et al. [121] utilized electro-click chemistry to modify boron-doped diamond (BDD) electrodes. The electro-click strategy enables precise control over the amount of Cu(I) catalyst and the loading of azide-terminated ferrocene on alkyne-terminated BDD electrodes. Compared with the chemical synthesis method, the electro-click approach offers advantages such as faster reaction kinetics, environmental friendliness, and the absence of chemical residues. Furthermore, the assessment technique inherent to electro-click chemistry is inherently uncomplicated, affording the direct interpretation of the reaction through the analysis of the cyclic voltammetry profile.

These reasons contribute to the ongoing popularity of the electro-click strategy.

3.3. Electro-Click Strategies for the Functionalization of Biosensor Interfaces

Before constructing biosensors, careful attention must be given to the functionalization strategies of the biosensor interfaces in order to meet diverse sensing requirements. The resulting interface should not only immobilize the biometric element in a stable manner, but also offer a selective and sensitive response. In this section, we will discuss the functionalization strategies for electrochemical biosensor interfaces and optical biosensor interfaces.

3.3.1. Electro-Click Strategies for the Functionalization of Electrochemical Biosensor Interfaces

Electrochemical biosensors have long been extensively utilized across various fields. These biosensors can generate sensing signals by monitoring changes in impedance, current, and dielectric properties when the target analyte is formed on the electrode surface. Numerous strategies exist for the modification of interfaces in electrochemical biosensors, encompassing approaches such as self-assembled monolayers, covalent immobilization, and electro-click methodologies, among others [122,123]. Concurrently, a diverse array of electrochemical biosensor variants is available. Notably, owing to its electrochemically mediated modifications and notable versatility, the electro-click strategy finds predominant utility within the domain of electrochemical biosensors. The functional modification strategies based on electro-click for electrochemical biosensor electrodes can be categorized into four parts: electrografting, electropolymerization, electrodeposition, and bipolar electrode methods.

Electrografting

The most commonly employed approach for modifying biosensing interfaces is electrografting [124,125]. Electro-click-mediated electrografting plays a crucial role in preparing controllable nanostructures, enhancing the sensor performance, and expanding the sensor functionalities [126]. In simple terms, azide and alkyne are grafted onto the biosensing interface and modifier, respectively, and then connected by the CuAAC electro-click reaction. For instance, Sciortino et al. [127] achieved a network structure of organic/inorganic hybrid products containing alkynes and polyethylene glycol azides with bifunctional groups through the electro-click reaction on an F-SnO_2 electrode. The composition and loading of these hybrid films can be adjusted, demonstrating the versatility of such hybrid coatings. Fenoy et al. [126] reported the synthesis of azide-derived organic electrochemical transistor monomers and applied them in a CuAAC reaction with a dibenzocyclooctyne-grafted thrombin-specific HD22 aptamer to achieve specific thrombin recognition. Also, Guerrero et al. [128] utilized ethynylated IgG bonded to azide-modified multi-walled carbon nanotube (MWCNT) electrodes to construct an electrochemical immunosensor for the cytokine interleukin 1b (IL-1b). The detection limit of this immunosensor was significantly improved to 5.2 pg/mL compared to the commercial kit. Effective coupling methods between interfaces are vital for achieving both sensitivity and selectivity. Therefore, we

employed cucurbituril- and azide-grafted graphene oxide to develop a novel functional nanomaterial as a biosensor interface for the detection of VEGF165 protein (Figure 8a) [129]. This interface demonstrated the simultaneous acquisition of sensitivity and selectivity, with a dynamic detection range of from 10 fg/mL to 1 ng/mL and a detection limit of 8 fg/mL. Electro-click-mediated electrografting enables the preparation of multipoint-specific electrode functionalization for multi-target biosensors on various materials. The examples discussed above clearly illustrate the potential of electro-click-mediated electrografting in expanding the capabilities of biosensor interfaces [130].

Electropolymerization

Electropolymerization (EP) refers to the network polymerization of solution components into a film when applying electrical stimulation through cyclic voltammetry (CV) [131]. This unique film structure enables the immobilization of functional molecules on or within the coating, making it suitable for combining with electro-click chemistry to create new functional biosensing interfaces. Rydzek et al. [131] developed self-assembled functional polymer films based on aniline and naphthalene using a one-pot method that involved simultaneous EP and electro-click functionalization. CV facilitated the oxidation of 4-azidoaniline and the reduction in Cu(II) ions, allowing for the simultaneous polymerization of the former and the CuAAC click reaction. For electropolymerization on conductive substrates, electrochemically mediated surface-initiated atom-transfer radical polymerization (SI-eATRP) offers a convenient approach to control polymer growth with low catalyst concentrations [132]. Wu et al. [133] achieved the fixation of sparse monomolecular membranes of ethynylphenyl on a carbon matrix through the electroreduction in aryldiazonium ions. They subsequently polymerized Poly(N-isopropylacrylamide) (PNIPAM) from the substrate in a one-pot solution containing an azide-derived initiator, PNIPAM, and a Cu catalyst (Figure 8b). The electro-reduction from Cu(II) to Cu(I) facilitated both the click reaction and SI-eATRP on the surface of the ethynylphenyl. This method is simple, convenient, and combines the advantages of electro-click chemistry and SI-eATRP.

Electrodeposition

Electrodeposition, as an electrochemical synthesis method based on solution-based synthesis, allows for the synthesis of different material types and the manipulation of various synthetic variables affecting morphology. It also enables the fabrication of uniform and tightly joined multi-junction electrodes through continuous multilayer deposition [134]. This feature proves particularly beneficial for synthesizing and functionalizing biosensing interfaces.

Conductive hydrogels, among various synthetic materials, have garnered attention from researchers. These hydrogels consist of conductive polymer networks formed by combining hydrogels with inherently conductive polymers. They offer a combination of biocompatibility, flexibility, high diffusivity, and conductivity [135,136]. Hydrogels can be prepared in specific forms on various substrates to suit the desired purpose. Hu et al. [137] described a method for coating chitosan hydrogel on a conductive surface using the electro-click-mediated electrodeposition technique. Chitosan was functionalized with azide or alkynyl groups, and a cathodic potential was applied to a gold chip to reduce Cu(II) ions to Cu(I) ions, catalyzing the CuAAC click reaction between the alkynyl chitosan and azide chitosan to form a conjugated chitosan hydrogel attached to the gold surface (Figure 8c). Experiments demonstrated the encapsulation of biomolecules within this hydrogel for biosensing purposes. Similarly, Choi et al. [138] electrodeposited PVA-based hydrogel on an indium tin oxide glass electrode using a Cu(I)-catalyzed CuAAC reaction with the reduction in Cu(II) ions. They found that embedding carbon nanotubes within the hydrogel enabled the deposition of thicker films due to the larger electrochemically active area provided by the carbon nanotubes.

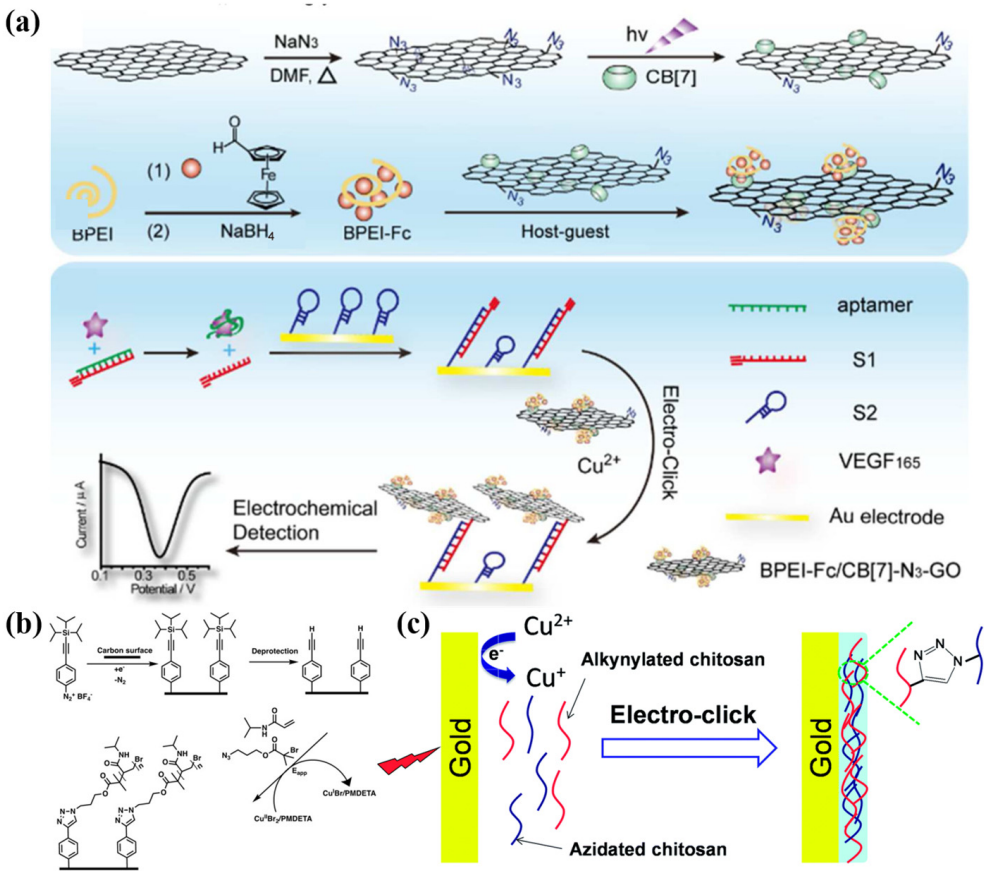

Figure 8. (**a**) Schematic of the BPEI-Fc/CB [7]-N_3-GO composite preparation and representation of the electro-click biosensing platform for VEGF165 analysis based on the composition. Reprinted with permission from [129], copyright 2017, *Anal Chem.* (**b**) Strategy for the preparation of H-Eth-Ar monolayers and grafting PNIPAM. Reprinted with permission from [133], copyright 2019, *ChemElectroChem*. (**c**) Schematic illustrating the "electro-click" chitosan hydrogel on a gold chip triggered by a negative potential that reduces Cu^{2+} to Cu^{+}. Reprinted with permission from [137], copyright 2014, *RSC Advances*.

Bipolar Electrodes

Bipolar electrodes (BPEs) can simultaneously perform anodic and cathodic reactions, making them a versatile electrochemical-reaction-driving mode and suitable as radio electrodes [139]. BPEs do not require electrical connection and can accommodate conductive materials of any shape and size, and even multiple materials at once (Figure 9a) [140]. These characteristics align well with electro-click chemistry (Figure 9b). The potential gradient at the BPE interface has been successfully utilized as a controllable template for forming molecular- or polymer-gradient materials, making it suitable for biomimetic materials or biosensor analysis equipment [141]. A study was conducted on the gradient modification of azide-functionalized conductive-polymer film using electrogenerated Cu(I) species on a bipolar electrode through an electroshock reaction in the presence of terminal alkyne [142]. This allowed the introduction of various gradient functions, such as gradient hydrophobicity/hydrophilicity and visible labeling, on the poly(3,4-ethylenedioxythiophene) (PEDOT) film to prepare the biosensing interface. In subsequent work, Zhou et al. [143] introduced a bipolar electrolytic micelle disruption (BEMD) system for shaping organic films. They created a U-shaped bipolar electrolysis system with an S-shaped potential gradient on the BPE, enabling the formation of a gradient film containing various organic compounds. This approach provided a novel idea and method for modifying organic membranes using the CuAAC electro-click reaction.

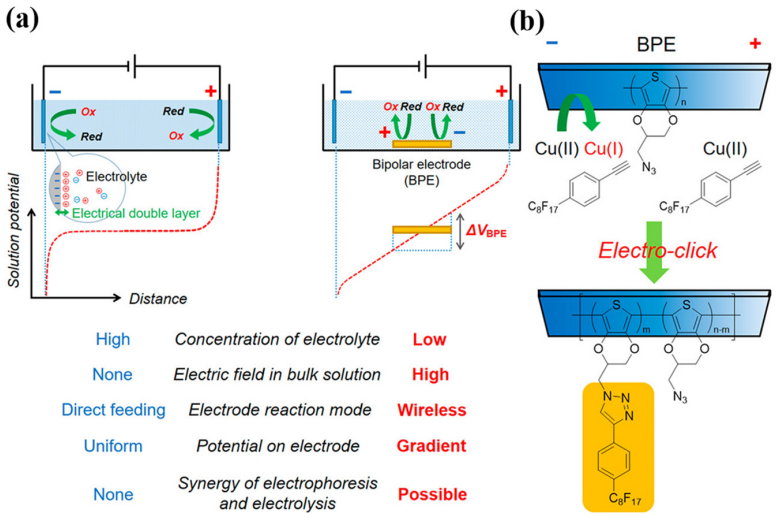

Figure 9. (**a**) Comparison of electrolytic systems for conventional and bipolar electrolysis. Red dotted line represents an ideal electric field generated between driving electrodes. (**b**) Scheme for the electro-click reaction of an azido-functionalized polymer film on a BPE with an alkyne derivative using an electrogenerated Cu(I) species. Reprinted with permission from [140], copyright 2019, *Acc Chem Res*.

Applications of Electro-Click Strategies in Electrochemical Biosensor Functionalization with Submicron Resolution

Numerous techniques are available for effecting functional alterations in biosensing interfaces, including single-molecule modification/deposition [144]. However, these methods seldom permit intricate modifications at the micron scale. Furthermore, they often exhibit constrained control over interface surfaces or necessitate costly equipment [145]. In stark contrast, a notable facet of electro-click chemistry, which entails electrochemical reactions, is its spatial selectivity. This distinctive attribute facilitates the precise functionalization of nanogaps, gradients, and microelectrodes, all achieved with submicron precision.

The utilization of NPs as fundamental building blocks has catalyzed the emergence of a novel category of nano-building materials, thereby illuminating a promising avenue for nano-gap functionalization. In a pioneering endeavor, Rydezk et al. [146] orchestrated a nanodevice with a high aspect ratio, selectively focused through covalent self-assembly via spatially arranged Cu(I)-catalyzed electro-click reactions. Employing dendritic iron oxide nanoparticles endowed with azide and alkyne functionalities as building blocks, they achieved a spatially orchestrated electro-click network structure. This method of NP functionalization proves highly adaptable and can be extrapolated to diverse nanoparticle varieties featuring clickable moieties. As such, the electro-click approach emerges as a sanguine instrument for seamlessly integrating covalent NPs into nanodevices, thereby beckoning forth prospects for biosensors and granular electronic devices [147].

The manipulation of physicochemical property gradients—marked by gradual spatial and temporal transitions—can substantially amplify the efficacy of catalyst and drug design, introducing novel analytical avenues of considerable import in solution and interface functionalization. Krabbenborg et al. [148] harnessed electro-click chemistry to fabricate a solution gradient, thereby enabling the high-throughput control and monitoring of the surface reactivity across spatial and temporal dimensions. By virtue of the solution gradient, finely adjustable and inherently predictable variations in the spatial concentration of chemically active species are achieved, engendering micron-scale surface gradients. In analogous fashion, Nicosia et al. [149] harnessed the CuAAC reaction to generate a monolayer on a glass surface flanked by platinum electrodes, effectively manipulating the gradient of the Cu(I) solution to effect microelectrode interface functionalization.

Beyond gradient-driven surface modification, the repertoire of electro-click chemistry extends to the direct functionalization of microelectrodes. Hansen et al. [150] directly

functionalized microelectrodes with PEDOT-N_3, showcasing a universally applicable and convenient strategy for diverse conductive-polymer functionalization. Notwithstanding the aforementioned applications, numerous prospects for submicron-resolution applications await exploration.

3.3.2. Electro-Click Strategies for the Functionalization of Optical Biosensor Interfaces

In recent times, the augmentation of optical biosensors using the electro-click approach has gained prominence. This development is attributed to the understanding that electron dynamics can arise not exclusively from direct electrochemical processes, but also from alternative energy excitations [151]. Consequently, as investigations into the interplay between photons and electrons advance, the electro-click strategy has found application within the realm of optical sensing [142,152]. Optical biosensors rely on measuring changes in the optical properties of the transducer surface when the analyte and recognition element form a complex [153]. They can be categorized as direct optical biosensors or indirect optical biosensors. While there are limited examples of optical biosensing interfaces prepared using electro-click chemistry, luminescent products prepared through electro-click have been identified. It is expected that similar functionalization strategies will be applied in the near future to prepare corresponding optical biosensors.

Direct optical biosensor signals depend on the complex formation on the biosensor interface. Shida et al. [142] used rhodamine-based acetylene as a visible indicator. After electroshock reaction on the bipolar electrode (Figure 10a), the polymer film was uniformly oxidized to the doped state, reducing the background absorption of PEDOT in the visible-light region. Consequently, the cathode part turned purple, allowing for naked-eye detection (Figure 10b). In addition to the existing direct optical sensor, Goll et al. [152] blended EDOT and branched 2,2′:3′,2″-terthiophene (3T) to form an EDOT-N_3 film that facilitated functional modification through an electro-click reaction. By altering the mixing ratio of the two materials, the optical properties exhibited significant changes that could be detected via infrared spectroscopy (Figure 10c).

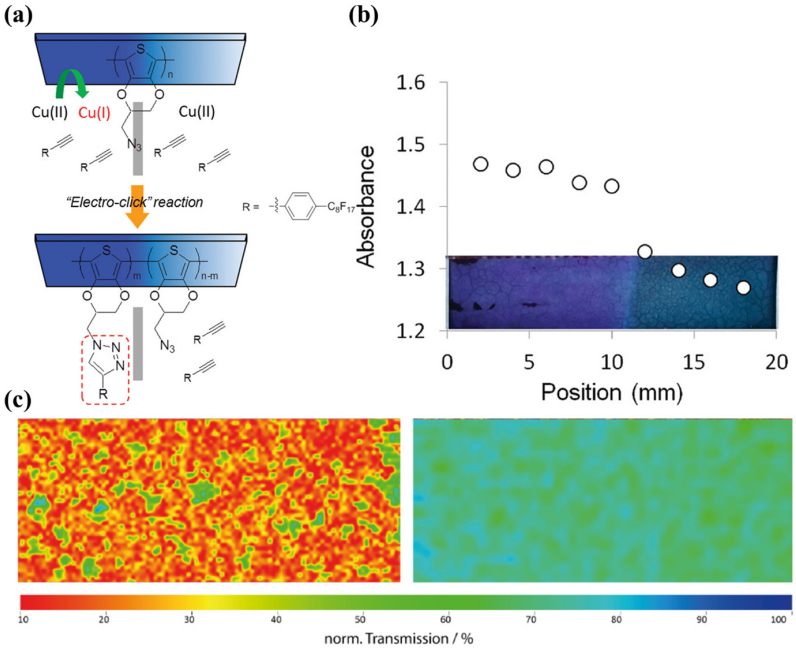

Figure 10. (**a**) Electro-click reaction of PEDOT-N_3 film and terminal alkyne using cathodically generated Cu(I) species. (**b**) Photograph of PEDOT-N_3 film gradually modified with rhodamine and the absorption profile (550 nm) across the film. Reprinted with permission from [142], copyright 2012, *ACS Macro Letters*. (**c**) IR mappings (bottom) of the azide band intensity at 2100 cm^{-1} of copolymer films deposited under potentiostatic control on gold in 0.1 M NBu_4PF_6/MeCN. Reprinted with permission from [152], copyright 2015, *Beilstein J Org Chem*.

Indirect optical biosensors commonly employ various labels, such as fluorophores, to detect and amplify signals. As early as 2008, Ku et al. [107] introduced the use of electro-click reactions to attach non-reactive fluorescent molecular patterns onto azide glass substrates (Figure 11a). This approach can be extended to enable the growth of any fluorescent molecule on an insulating substrate, forming a direct covalent bond beneath the microelectrode. The F-SnO_2 coating developed by Sciortino et al. [127] using the aforementioned electro-click reaction exhibited notable differences in fluorescence spectra when loaded with 4,4-Difluoro-8-(4-trimethylsilylethynylphenyl)-1,3,5,7-tetramethyl-2,6-diethyl-4-bora-3a,4a-diaza-s-indacene(BODIPY) (Figure 11b). This method also proves to be a viable approach for indirect optical biosensors. Coceancigh et al. [154] employed electrochemically assisted CuAAC to precisely control the inner surface of poly(ethylene terephthalate) (PET) track-etched pores. In this process, the ethynyl groups within the etched holes were first modified via the amidation of the surface-COOH groups. Subsequently, a solution containing copper (II) and azide-labeled fluorescent dye was introduced and sandwiched between gold electrodes (Figure 11c). Rydzek et al. [155] harnessed the electro-click reaction methodology to fabricate a thin film atop a gold electrode. Variations in the pH induced distinct electrostatic-repulsion patterns between PAA-Alk moieties, thereby governing the structural attributes of the resultant film. These disparities in the film structure were anticipated to manifest as discernible divergences in fluorescence responses. As a result, the fluorescent group could be directly immobilized onto the membrane. Furthermore, materials such as CNTs, CDs, and luminol exhibit light-specific properties [45,63,110]. If they can be utilized for modification, then a broader range of functional optical biosensor interfaces could be developed to meet diverse requirements.

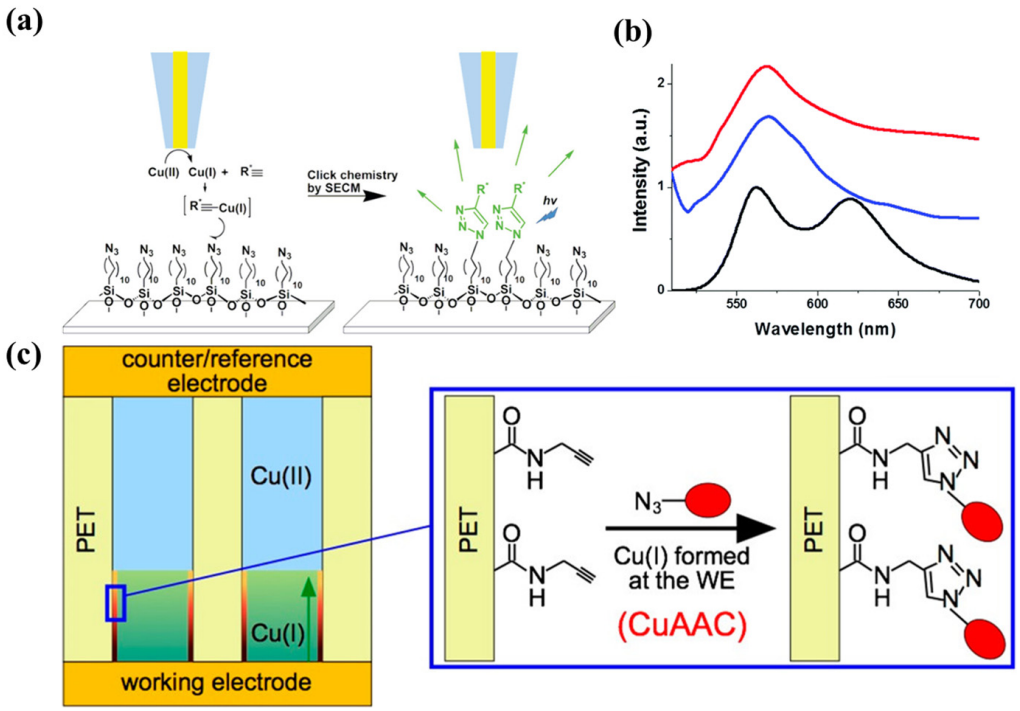

Figure 11. (**a**) Local reduction of Cu(II) to Cu(I) at a gold microelectrode (left) and immobilization of acetylene fluorophore derivatives onto a glass. Reprinted with permission from [107], copyright 2008, *Journal of the American Chemical Society*. (**b**) Fluorescence spectra in the dry state (λ_{exc} at 480 nm) of BODIPY (black line), drop-casted bodipy-loaded hybridosome (blue line), and an electro-clicked film based on BODIPY-loaded hybridosomes (red line). Reprinted with permission from [127], copyright 2018, *Phys Chem Chem Phys*. (**c**) Electrochemically controlled pore modification based on CuAAC. Reprinted with permission from [154], copyright 2017, *Langmuir*.

3.3.3. Limits of Electro-Click Strategies for the Functionalization of Biosensor Interfaces

Electro-click chemistry offers an expedient, versatile, and facile approach to biosensing interface functionalization; nevertheless, it is not without its imperfections. Several challenges persist, warranting researchers' dedicated efforts. Within the realm of biosensors, a paramount concern in the electro-click methodology is the retention of copper ions (Cu(II)/Cu(I)) during functionalization, which could potentially impede biomolecular activity. Cu(II) might catalyze the production of reactive oxygen species at the biosensing interface, engendering lipid peroxidation, protein oxidation, and DNA degradation [156]. Cu(I) is highly thiophilic and can directly damage the Fe-S-cluster-containing enzyme modifiers in the biosensing interface [157]. Schaaf et al. [158] ventured to ameliorate the Cu(II) influence via EDTA, yielding commendable outcomes. Contemporary endeavors, such as those by Cheng et al. [159], persist in deploying EDTA overdosing to tackle this conundrum. Beyond chemical mitigation, physical adsorption emerges as an effective countermeasure against Cu(II). In this vein, Liu et al. [160] prepared triethanolamine-GO nanosheets to robustly adsorb Cu(II), displaying an elevated equilibrium capacity even at higher initial Cu(II) concentrations.

Early forays into electro-click applications also confronted challenges in characterizing functionalized biosensing interfaces. Evolving scientific and technological advancements have enriched the characterization methodologies, enhancing precision and deepening researchers' appreciation for the electro-click paradigm. Presently, indirect characterization techniques, spanning SEM [104,119,127], TEM [104,127], XRD [104], BET [104], fluorescence [104,127], CV [119,120,127,128,131], and EIS [128], discerningly probe interfacial substance connections. Complementary to these indirect avenues, polarization-modulated infrared-reflectance-absorption spectroscopy (PM-IRRAS) [119,120], XPS [104,131,142], and EDS [104,127,142] have emerged as more direct means of elucidating reactions via element- or chemical-group alterations at electrode surfaces. It is firmly believed that future endeavors will engender a proliferation of characterization methods, augmenting researchers' arsenal for scrutinizing electro-click-functionalized biosensing interfaces.

The widespread adoption of the electro-click reaction rests on its attributes of expeditious reaction kinetics, ecological benignity, and minimal pollution. However, investigations into the recycling and reutilization of electro-click-functionalized biosensing interfaces have remained relatively sparse, casting a spotlight on a nascent concern for future inquiry. Encouragingly, select researchers have delved into recycling experiments concerning electro-click-functionalized biosensors. For instance, Fomo et al. [106] demonstrated the potential for electrode reuse by washing it with deionized water after sample detection, subsequently reemploying the electrode with negligible alteration in DPSV voltammograms, attesting to the sensor viability. Likewise, Qi et al. [117] exhibited a stable immunosensor retention for 15 days, with the subsequent detection revealing a commendable 88% retention of the initial steady-state current. These instances provide inspiring precedents. Thus, within the domain of electro-click-functionalized biosensing interfaces, the focus must expand beyond novel modification methodologies, encompassing heightened attention toward interface recyclability and, building upon this foundation, the exploration of straightforward recovery protocols. In general, the journey toward electro-click-modified-functionalized biosensing interfaces stretches ahead, necessitating persistent exploration and innovation.

4. Conclusions

In summary, we have comprehensively examined the different strategies for functionalizing biosensing interfaces, encompassing nanomaterials, small molecules, biomacromolecules, and cell-mediated interfacial regulations. We have also delved into the process of transforming identified elements into signals, imparting functionality to the sensor, and enhancing its performance.

Among the various functionalization strategies for biosensing interfaces, click chemistry stands out due to its advantages of rapidity, selectivity, and low pollution. We have elucidated the origins and principles of click chemistry, with CuAAC serving as an exem-

plar, highlighting its advantages. In the realm of electrochemical biosensors, the use of click-chemistry-based modifications on the sensing interface offers improved stability and convenience, leading to more discernible electrochemical signals. For optical biosensors, the modified sensing interface not only generates optical signals in response to the target analyte, but also amplifies the signal through the incorporated materials, thereby bolstering the reliability of the sensing outcomes. Within this domain, electro-click chemistry emerges as an environmentally friendly, swift, and convenient approach, surpassing traditional click chemistry in terms of functionalizing biosensing interfaces. We have summarized the research and application progress of electro-click chemistry in functionalizing electrochemical biosensors and optical sensors. While there may be fewer corresponding examples in optical biosensors, drawing from related literature, this review has identified potential examples that can be utilized for constructing optical biosensor interfaces.

This review provides a fresh perspective for the development of novel functional biosensing interface strategies. Moreover, the expansion of biosensing systems based on electro-click chemistry will contribute to the selection of materials and the advancement of strategies. Ultimately, this will broaden the applications of biosensors across diverse fields, such as chemistry, agriculture, food science, clinical diagnostics, pharmaceuticals, and environmental analysis.

Author Contributions: Conceptualization, T.W.; methodology, T.W.; investigation, F.W.; writing—original draft preparation, F.W., Y.X. and W.Z.; writing—review and editing, T.W., F.W., Y.X. and W.Z. All authors have read and agreed to the published version of the manuscript.

Funding: This work was supported by the National Natural Science Foundation of China (Grant No. 22074064).

Institutional Review Board Statement: Not applicable.

Informed Consent Statement: Not applicable.

Data Availability Statement: No new data were created.

Conflicts of Interest: The authors declare no conflict of interest.

Abbreviations

Acronym	Definition
GO	Graphene oxide
Exo III	Exonuclease III
HP1 and HP2	Hairpin probes
PtNFS-GO	Flower-like Pt-graphene oxide
8-OHdG	8-hydroxy-2′-deoxyguanosine
rGO	Reduced graphene oxide
LOD	Low detection limit
Fe/N-C	N-doped porous-carbon-containing Fe
ECL	Electrochemiluminescence
SWCNTs	Single-walled carbon nanotubes
MWCNTs	Multi-walled carbon nanotubes
NIR	Near-infrared
PDAC	Pancreatic ductal adenocarcinoma
EDOT	3,4-ethylenedioxythiophene
PEDOT	Poly(3,4-ethylenedioxythiophene)
Au@Pt	Au@Pt nanocrystals
FNAs	Framework nucleic acids
E. coli O157:H7	Escherichia coli O157:H7
AgNCs	Silver nanoclusters
SC	Scopoletin
AR	Amplex Red
ATPA	Adenosine triphosphate aptamer
ATP	Adenosine triphosphate
DsDNA	Double-stranded DNA
HDNA	Hairpin DNA
SsDNA	Single-stranded DNA
NPs	Nanoparticles
RBD	Receptor-binding domain
HSA	Human serum albumin
SRB	Sulfate-reducing bacteria
RBC	Red blood cell
PLNPs	Persistent luminescent nanophosphors
MCF	Mesoporous carbon framework
HEMA	Hydroxyethyl methacrylate
DEAEMA	2-(diethylamino)ethyl methacrylate
SPE	Gold screen-printed electrodes
AFB1	Aflatoxin B1
OTA	Ochratoxin A
NP	Nucleocapsid protein
IgG	Immunoglobulin G
CuAAC	Cu(I)-catalyzed alkyne–azide cycloaddition
CXCL7	Chemokine (C-X-C motif) ligand 7

Acronym	Definition	Acronym	Definition
GSH	Glutathione	GO-N_3	Azide-co-functionalized graphene oxide
PSA	Prostate-specific antigen	CDs	Carbon dots
PCa	Prostate cancer	CDs-DNA	Carbon-dot-labeled DNA
GDY	Graphdiyne	FRET	Fluorescence resonance energy transfer
C-MIPs	C-reactive-molecular-imprinted polymers	CEA	Carcinoembryonic antigen
HRP	Horseradish peroxidase	MspA	Mycobacterium smegmatis porin A
ROS	Reactive oxygen species	DBCO	Dibenzocyclooctyne
O_2^-	Superoxide radicals	PAA	Poly(acrylic acid)
Au/VO_2	Gold-loaded 2D VO_2 nanobelts	PAAalk	Poly(acrylic acid) multilayers with alkynyl
RET	Resonance energy transfer	PAAaz	Poly(acrylic acid) multilayers with azide
MIT	Molecular-imprinting technology	BDD	Boron-doped diamond
HER-2	Human epidermal growth factor receptor 2	EP	Electropolymerization
HOCl	Hypochlorous acid	CV	Cyclic voltammetry
$OONO^-$	Peroxynitrite	SI-eATRP	Surface-initiated atom-transfer radical polymerization
GOx	Glucose oxidase	PNIPAM	Poly(N-isopropylacrylamide)
MG	Mxene–graphene	BPEs	Bipolar electrodes
CHI	Chitosan	PEDOT	Poly(3,4-ethylenedioxythiophene)
Co_3O_4 @ MCF	Cobalt oxide-loaded mesoporous carbon framework	BEMD	Bipolar electrolytic micelle disruption
AChE	Acetylcholinesterase	3T	2,2′:3′,2″-terthiophene
pp	Plasma-polymerized	PET	Poly(ethylene terephthalate)
FDNA	Framework DNA	BODIPY	4,4-Difluoro-8-(4-trimethylsilylethynylphenyl) -1,3,5,7-tetramethyl-2,6-diethyl-4-bora-3a, 4a-diaza-s-indacene

References

1. Walther, B.K.; Dinu, C.Z.; Guldi, D.M.; Sergeyev, V.G.; Creager, S.E.; Cooke, J.P.; Guiseppi-Elie, A. Nanobiosensing with graphene and carbon quantum dots: Recent advances. *Mater. Today* **2020**, *39*, 23–46.
2. Singh, S.; Kumar, V.; Dhanjal, D.S.; Datta, S.; Prasad, R.; Singh, J. Biological biosensors for monitoring and diagnosis. In *Microbial Biotechnology*; Springer: Berlin/Heidelberg, Germany, 2020; pp. 317–335.
3. Cheng, Z.; Wei, J.; Gu, L.; Zou, L.; Wang, T.; Chen, L.; Li, Y.; Yang, Y.; Li, P. DNAzyme-based biosensors for mercury (II) detection: Rational construction, advances and perspectives. *J. Hazard. Mater.* **2022**, *431*, 128606.
4. Gosai, A.; Khondakar, K.R.; Ma, X.; Ali, M.A. Application of Functionalized Graphene Oxide Based Biosensors for Health Monitoring: Simple Graphene Derivatives to 3D Printed Platforms. *Biosensors* **2021**, *11*, 384. [PubMed]
5. Bandodkar, A.J.; Wang, J. Non-invasive wearable electrochemical sensors: A review. *Trends Biotechnol.* **2014**, *32*, 363–371.
6. Zhao, Q.; Zhang, Q.; Sun, Y.; Liu, Y.; Lu, H.; Fan, X.; Wang, H.; Zhang, Y.; Wang, H. Design synthesis of a controllable flower-like Pt-graphene oxide architecture through electrostatic self-assembly for DNA damage biomarker 8-hydroxy-2′-deoxyguanosine biosensing research. *Analyst* **2018**, *143*, 3619–3627. [PubMed]
7. Levien, M.; Farka, Z.; Pastucha, M.; Skládal, P.; Nasri, Z.; Weltmann, K.-D.; Fricke, K. Functional plasma-polymerized hydrogel coatings for electrochemical biosensing. *Appl. Surf. Sci.* **2022**, *584*, 152511.
8. Kolb, H.C.; Finn, M.G.; Sharpless, K.B. Click Chemistry: Diverse Chemical Function from a Few Good Reactions. *Angew. Chem. Int. Ed.* **2001**, *40*, 2004–2021.
9. Hein, J.E.; Fokin, V.V. Copper-catalyzed azide–alkyne cycloaddition (CuAAC) and beyond: New reactivity of copper (I) acetylides. *Chem. Soc. Rev.* **2010**, *39*, 1302–1315.
10. Deng, Y.; Shavandi, A.; Okoro, O.V.; Nie, L. Alginate modification via click chemistry for biomedical applications. *Carbohydr. Polym.* **2021**, *270*, 118360.
11. Shi, W.; Tang, F.; Ao, J.; Yu, Q.; Liu, J.; Tang, Y.; Jiang, B.; Ren, X.; Huang, H.; Yang, W. Manipulating the Click Reactivity of Dibenzoazacyclooctynes: From Azide Click Component to Caged Acylation Reagent by Silver Catalysis. *Angew. Chem. Int. Ed.* **2020**, *132*, 20112–20116.
12. Yoon, H.Y.; Lee, D.; Lim, D.K.; Koo, H.; Kim, K. Copper-Free Click Chemistry: Applications in Drug Delivery, Cell Tracking, and Tissue Engineering. *Adv. Mater.* **2022**, *34*, 2107192.
13. Kondengadan, S.M.; Bansal, S.; Yang, C.; Liu, D.; Fultz, Z.; Wang, B. Click chemistry and drug delivery: A bird's-eye view. *Acta Pharm. Sin. B* **2022**, *13*, 1990–2016. [CrossRef]
14. Fitzgerald, P.R.; Paegel, B.M. DNA-encoded chemistry: Drug discovery from a few good reactions. *Chem. Rev.* **2020**, *121*, 7155–7177. [CrossRef]
15. Kim, E.; Koo, H. Biomedical applications of copper-free click chemistry: In vitro, in vivo, and ex vivo. *Chem. Sci.* **2019**, *10*, 7835–7851. [CrossRef]

16. Rydzek, G.; Ji, Q.; Li, M.; Schaaf, P.; Hill, J.P.; Boulmedais, F.; Ariga, K. Electrochemical nanoarchitectonics and layer-by-layer assembly: From basics to future. *Nano Today* **2015**, *10*, 138–167. [CrossRef]
17. Deo, K.A.; Jaiswal, M.K.; Abasi, S.; Lokhande, G.; Bhunia, S.; Nguyen, T.-U.; Namkoong, M.; Darvesh, K.; Guiseppi-Elie, A.; Tian, L. Nanoengineered Ink for Designing 3D Printable Flexible Bioelectronics. *ACS Nano* **2022**, *16*, 8798–8811. [CrossRef]
18. Zhang, W.; Zhu, S.; Luque, R.; Han, S.; Hu, L.; Xu, G. Recent development of carbon electrode materials and their bioanalytical and environmental applications. *Chem. Soc. Rev.* **2016**, *45*, 715–752.
19. Lopez, A.; Liu, J. Covalent and Noncovalent Functionalization of Graphene Oxide with DNA for Smart Sensing. *Adv. Intell. Syst.* **2020**, *2*, 2000123. [CrossRef]
20. Georgakilas, V.; Tiwari, J.N.; Kemp, K.C.; Perman, J.A.; Bourlinos, A.B.; Kim, K.S.; Zboril, R. Noncovalent functionalization of graphene and graphene oxide for energy materials, biosensing, catalytic, and biomedical applications. *Chem. Rev.* **2016**, *116*, 5464–5519.
21. Zhang, M.; Li, Y.; Su, Z.; Wei, G. Recent advances in the synthesis and applications of graphene–polymer nanocomposites. *Polym. Chem.* **2015**, *6*, 6107–6124. [CrossRef]
22. Liu, B.; Salgado, S.; Maheshwari, V.; Liu, J. DNA adsorbed on graphene and graphene oxide: Fundamental interactions, desorption and applications. *Curr. Opin. Colloid. Interface Sci.* **2016**, *26*, 41–49.
23. Szunerits, S.; Boukherroub, R. Graphene-based bioelectrochemistry and bioelectronics: A concept for the future? *Curr. Opin. Electrochem.* **2018**, *12*, 141–147. [CrossRef]
24. Vivaldi, F.M.; Dallinger, A.; Bonini, A.; Poma, N.; Sembranti, L.; Biagini, D.; Salvo, P.; Greco, F.; Di Francesco, F. Three-dimensional (3D) laser-induced graphene: Structure, properties, and application to chemical sensing. *ACS Appl. Mater. Interfaces* **2021**, *13*, 30245–30260. [CrossRef]
25. Wei, T.; Dai, Z.; Lin, Y.; Du, D. Electrochemical Immunoassays Based on Graphene: A Review. *Electroanalysis* **2016**, *28*, 4–12. [CrossRef]
26. Perrozzi, F.; Prezioso, S.; Ottaviano, L. Graphene oxide: From fundamentals to applications. *J. Phys. Condens. Matter* **2014**, *27*, 013002. [CrossRef]
27. Gao, L.; Lian, C.; Zhou, Y.; Yan, L.; Li, Q.; Zhang, C.; Chen, L.; Chen, K. Graphene oxide-DNA based sensors. *Biosens. Bioelectron.* **2014**, *60*, 22–29. [CrossRef] [PubMed]
28. Iwe, I.; Li, Z.; Huang, J. Graphene oxide and enzyme-assisted dual-cycling amplification method for sensitive fluorometric determination of DNA. *Mikrochim. Acta* **2019**, *186*, 716. [CrossRef]
29. Wei, T.; Chen, Y.; Tu, W.; Lan, Y.; Dai, Z. A phosphomolybdic acid anion probe-based label-free, stable and simple electrochemical biosensing platform. *Chem. Commun.* **2014**, *50*, 9357–9360. [CrossRef]
30. Shamsipur, M.; Molaei, K.; Molaabasi, F.; Hosseinkhani, S.; Taherpour, A.; Sarparast, M.; Moosavifard, S.E.; Barati, A. Aptamer-based fluorescent biosensing of adenosine triphosphate and cytochrome c via aggregation-induced emission enhancement on novel label-free DNA-capped silver nanoclusters/graphene oxide nanohybrids. *ACS Appl. Mater. Interfaces* **2019**, *11*, 46077–46089. [CrossRef] [PubMed]
31. Asefifeyzabadi, N.; Holland, T.E.; Sivakumar, P.; Talapatra, S.; Senanayake, I.M.; Goodson, B.M.; Shamsi, M.H. Sequence-Independent DNA Adsorption on Few-Layered Oxygen-Functionalized Graphene Electrodes: An Electrochemical Study for Biosensing Application. *Biosensors* **2021**, *11*, 273. [CrossRef] [PubMed]
32. Pena-Bahamonde, J.; Nguyen, H.N.; Fanourakis, S.K.; Rodrigues, D.F. Recent advances in graphene-based biosensor technology with applications in life sciences. *J. Nanobiotechnology* **2018**, *16*, 75. [PubMed]
33. Qiu, L.; Li, D.; Cheng, H.M. Structural Control of Graphene-Based Materials for Unprecedented Performance. *ACS Nano* **2018**, *12*, 5085–5092. [CrossRef]
34. Cao, S.H.; Li, L.H.; Wei, W.Y.; Feng, Y.; Jiang, W.L.; Wang, J.L.; Zhang, X.P.; Cai, S.H.; Chen, Z. A label-free and ultrasensitive DNA impedimetric sensor with enzymatic and electrical dual-amplification. *Analyst* **2019**, *144*, 4175–4179. [CrossRef] [PubMed]
35. Ali, M.A.; Hu, C.; Jahan, S.; Yuan, B.; Saleh, M.S.; Ju, E.; Gao, S.J.; Panat, R. Sensing of COVID-19 Antibodies in Seconds via Aerosol Jet Nanoprinted Reduced-Graphene-Oxide-Coated 3D Electrodes. *Adv. Mater.* **2021**, *33*, 2006647. [CrossRef]
36. Maduraiveeran, G.; Jin, W. Nanomaterials based electrochemical sensor and biosensor platforms for environmental applications. *Trends Environ. Anal.* **2017**, *13*, 10–23.
37. Guan, H.; Zhong, T.; He, H.; Zhao, T.; Xing, L.; Zhang, Y.; Xue, X. A self-powered wearable sweat-evaporation-biosensing analyzer for building sports big data. *Nano Energy* **2019**, *59*, 754–761. [CrossRef]
38. Gao, J.W.; Chen, M.M.; Wen, W.; Zhang, X.; Wang, S.; Huang, W.H. Au-Luminol-decorated porous carbon nanospheres for the electrochemiluminescence biosensing of MUC1. *Nanoscale* **2019**, *11*, 16860–16867. [CrossRef] [PubMed]
39. Tian, H.; Tan, B.; Dang, X.; Zhao, H. Enhanced Electrochemiluminescence Detection for Hydrogen Peroxide Using Peroxidase-Mimetic Fe/N-Doped Porous Carbon. *J. Electrochem. Soc.* **2019**, *166*, 1594–1601. [CrossRef]
40. Safaee, M.M.; Gravely, M.; Roxbury, D. A Wearable Optical Microfibrous Biomaterial with Encapsulated Nanosensors Enables Wireless Monitoring of Oxidative Stress. *Adv. Funct. Mater.* **2021**, *31*, 2006254. [CrossRef]
41. Saheb, A.; Janata, J.; Josowicz, M. Reference electrode for ionic liquids. *Electroanalysis* **2006**, *18*, 405–409. [CrossRef]
42. Iijima, S.; Ichihashi, T. Single-shell carbon nanotubes of 1-nm diameter. *Nature* **1993**, *363*, 603–605.
43. Iijima, S. Helical microtubules of graphitic carbon. *Nature* **1991**, *354*, 56–58. [CrossRef]

44. Gooding, J.J. Nanostructuring electrodes with carbon nanotubes: A review on electrochemistry and applications for sensing. *Electrochim. Acta* **2005**, *50*, 3049–3060.
45. Lew, T.T.S.; Koman, V.B.; Silmore, K.S.; Seo, J.S.; Gordiichuk, P.; Kwak, S.Y.; Park, M.; Ang, M.C.; Khong, D.T.; Lee, M.A.; et al. Real-time detection of wound-induced H_2O_2 signalling waves in plants with optical nanosensors. *Nat. Plants* **2020**, *6*, 404–415.
46. Bhattacharya, S.; Gong, X.; Wang, E.; Dutta, S.K.; Caplette, J.R.; Son, M.; Nguyen, F.T.; Strano, M.S.; Mukhopadhyay, D. DNA-SWCNT Biosensors Allow Real-Time Monitoring of Therapeutic Responses in Pancreatic Ductal Adenocarcinoma. *Cancer Res.* **2019**, *79*, 4515–4523. [PubMed]
47. Harvey, J.D.; Williams, R.M.; Tully, K.M.; Baker, H.A.; Shamay, Y.; Heller, D.A. An in Vivo Nanosensor Measures Compartmental Doxorubicin Exposure. *Nano Lett.* **2019**, *19*, 4343–4354.
48. Salem, D.P.; Gong, X.; Liu, A.T.; Akombi, K.; Strano, M.S. Immobilization and Function of nIR-Fluorescent Carbon Nanotube Sensors on Paper Substrates for Fluidic Manipulation. *Anal. Chem.* **2020**, *92*, 916–923.
49. Meng, L.; Turner, A.P.F.; Mak, W.C. Tunable 3D nanofibrous and bio-functionalised PEDOT network explored as a conducting polymer-based biosensor. *Biosens. Bioelectron.* **2020**, *159*, 112181.
50. Zhao, Z.; Chen, H.; Cheng, Y.; Huang, Z.; Wei, X.; Feng, J.; Cheng, J.; Mugo, S.M.; Jaffrezic-Renault, N.; Guo, Z. Electrochemical aptasensor based on electrodeposited poly (3, 4-ethylenedioxythiophene)-graphene oxide coupled with Au@ Pt nanocrystals for the detection of 17β-estradiol. *Microchim. Acta* **2022**, *189*, 178.
51. Zhu, F.; Bian, X.; Zhang, H.; Wen, Y.; Chen, Q.; Yan, Y.; Li, L.; Liu, G.; Yan, J. Controllable design of a nano-bio aptasensing interface based on tetrahedral framework nucleic acids in an integrated microfluidic platform. *Biosens. Bioelectron.* **2021**, *176*, 112943.
52. Jia, Y.; Yi, X.; Li, Z.; Zhang, L.; Yu, B.; Zhang, J.; Wang, X.; Jia, X. Recent advance in biosensing applications based on two-dimensional transition metal oxide nanomaterials. *Talanta* **2020**, *219*, 121308.
53. Fan, Y.; Liu, S.; Yi, Y.; Rong, H.; Zhang, J. Catalytic Nanomaterials toward Atomic Levels for Biomedical Applications: From Metal Clusters to Single-Atom Catalysts. *ACS Nano* **2021**, *15*, 2005–2037.
54. Zhou, W.; Saran, R.; Liu, J. Metal sensing by DNA. *Chem. Rev.* **2017**, *117*, 8272–8325.
55. Fan, D.; Shang, C.; Gu, W.; Wang, E.; Dong, S. Introducing Ratiometric Fluorescence to MnO_2 Nanosheet-Based Biosensing: A Simple, Label-Free Ratiometric Fluorescent Sensor Programmed by Cascade Logic Circuit for Ultrasensitive GSH Detection. *ACS Appl. Mater. Interfaces* **2017**, *9*, 25870–25877.
56. Yadav, V.; Roy, S.; Singh, P.; Khan, Z.; Jaiswal, A. 2D MoS(2)-Based Nanomaterials for Therapeutic, Bioimaging, and Biosensing Applications. *Small* **2019**, *15*, 1803706.
57. Yan, R.; Lu, N.; Han, S.; Lu, Z.; Xiao, Y.; Zhao, Z.; Zhang, M. Simultaneous detection of dual biomarkers using hierarchical MoS_2 nanostructuring and nano-signal amplification-based electrochemical aptasensor toward accurate diagnosis of prostate cancer. *Biosens. Bioelectron.* **2022**, *197*, 113797.
58. Han, H.-H.; Tian, H.; Zang, Y.; Sedgwick, A.C.; Li, J.; Sessler, J.L.; He, X.-P.; James, T.D. Small-molecule fluorescence-based probes for interrogating major organ diseases. *Chem. Soc. Rev.* **2021**, *50*, 9391–9429.
59. Cui, M.; Che, Z.; Gong, Y.; Li, T.; Hu, W.; Wang, S. A graphdiyne-based protein molecularly imprinted biosensor for highly sensitive human C-reactive protein detection in human serum. *Chem. Eng. J.* **2022**, *431*, 133455.
60. Salimian, R.; Kékedy-Nagy, L.; Ferapontova, E.E. Specific Picomolar Detection of a Breast Cancer Biomarker HER-2/neu Protein in Serum: Electrocatalytically Amplified Electroanalysis by the Aptamer/PEG-Modified Electrode. *ChemElectroChem* **2017**, *4*, 872–879.
61. Zhang, L.; Xiao, X.; Xu, Y.; Chen, D.; Chen, J.; Ma, Y.; Dai, Z.; Zou, X. Electrochemical assay for continuous monitoring of dynamic DNA methylation process. *Biosens. Bioelectron.* **2018**, *100*, 184–191. [PubMed]
62. Tian, X.; Murfin, L.C.; Wu, L.; Lewis, S.E.; James, T.D. Fluorescent small organic probes for biosensing. *Chem. Sci.* **2021**, *12*, 3406–3426.
63. Ma, X.; Gao, W.; Du, F.; Yuan, F.; Yu, J.; Guan, Y.; Sojic, N.; Xu, G. Rational Design of Electrochemiluminescent Devices. *Acc. Chem. Res.* **2021**, *54*, 2936–2945. [PubMed]
64. Ma, C.; Cao, Y.; Gou, X.; Zhu, J.J. Recent Progress in Electrochemiluminescence Sensing and Imaging. *Anal. Chem.* **2020**, *92*, 431–454. [PubMed]
65. Zhang, Y.; Xu, J.; Zhou, S.; Zhu, L.; Lv, X.; Zhang, J.; Zhang, L.; Zhu, P.; Yu, J. DNAzyme-Triggered Visual and Ratiometric Electrochemiluminescence Dual-Readout Assay for Pb(II) Based on an Assembled Paper Device. *Anal. Chem.* **2020**, *92*, 3874–3881.
66. Guo, J.; Xie, M.; Du, P.; Liu, Y.; Lu, X. Signal Amplification Strategy Using Atomically Gold-Supported VO(2) Nanobelts as a Co-reaction Accelerator for Ultrasensitive Electrochemiluminescent Sensor Construction Based on the Resonance Energy Transfer Platform. *Anal. Chem.* **2021**, *93*, 10619–10626.
67. Wu, K.; Zheng, Y.; Chen, R.; Zhou, Z.; Liu, S.; Shen, Y.; Zhang, Y. Advances in electrochemiluminescence luminophores based on small organic molecules for biosensing. *Biosens. Bioelectron.* **2023**, *223*, 115031.
68. Wu, X.; Li, Z.; Yang, L.; Han, J.; Han, S. A self-referenced nanodosimeter for reaction based ratiometric imaging of hypochlorous acid in living cells. *Chem. Sci.* **2013**, *4*, 460–467.
69. Jia, X.; Chen, Q.; Yang, Y.; Tang, Y.; Wang, R.; Xu, Y.; Zhu, W.; Qian, X. FRET-Based Mito-Specific Fluorescent Probe for Ratiometric Detection and Imaging of Endogenous Peroxynitrite: Dyad of Cy3 and Cy5. *J. Am. Chem. Soc.* **2016**, *138*, 10778–10781. [PubMed]

70. Gu, K.; Xu, Y.; Li, H.; Guo, Z.; Zhu, S.; Zhu, S.; Shi, P.; James, T.D.; Tian, H.; Zhu, W.H. Real-Time Tracking and In Vivo Visualization of beta-Galactosidase Activity in Colorectal Tumor with a Ratiometric Near-Infrared Fluorescent Probe. *J. Am. Chem. Soc.* **2016**, *138*, 5334–5340. [PubMed]
71. Murfin, L.C.; Weber, M.; Park, S.J.; Kim, W.T.; Lopez-Alled, C.M.; McMullin, C.L.; Pradaux-Caggiano, F.; Lyall, C.L.; Kociok-Kohn, G.; Wenk, J.; et al. Azulene-Derived Fluorescent Probe for Bioimaging: Detection of Reactive Oxygen and Nitrogen Species by Two-Photon Microscopy. *J. Am. Chem. Soc.* **2019**, *141*, 19389–19396.
72. Chen, H.; Tang, Y.; Ren, M.; Lin, W. Single near-infrared fluorescent probe with high- and low-sensitivity sites for sensing different concentration ranges of biological thiols with distinct modes of fluorescence signals. *Chem. Sci.* **2016**, *7*, 1896–1903.
73. Jiao, Y.; Yin, J.; He, H.; Peng, X.; Gao, Q.; Duan, C. Conformationally Induced Off-On Cell Membrane Chemosensor Targeting Receptor Protein-Tyrosine Kinases for in Vivo and in Vitro Fluorescence Imaging of Cancers. *J. Am. Chem. Soc.* **2018**, *140*, 5882–5885. [CrossRef]
74. Long, L.; Huang, M.; Wang, N.; Wu, Y.; Wang, K.; Gong, A.; Zhang, Z.; Sessler, J.L. A Mitochondria-Specific Fluorescent Probe for Visualizing Endogenous Hydrogen Cyanide Fluctuations in Neurons. *J. Am. Chem. Soc.* **2018**, *140*, 1870–1875. [CrossRef] [PubMed]
75. Sassolas, A.; Blum, L.J.; Leca-Bouvier, B.D. Immobilization strategies to develop enzymatic biosensors. *Biotechnol. Adv.* **2012**, *30*, 489–511. [PubMed]
76. Gu, H.; Xing, Y.; Xiong, P.; Tang, H.; Li, C.; Chen, S.; Zeng, R.; Han, K.; Shi, G. Three-Dimensional Porous $Ti_3C_2T_x$ MXene–Graphene Hybrid Films for Glucose Biosensing. *ACS Appl. Nano Mater.* **2019**, *2*, 6537–6545. [CrossRef]
77. Dhanjai; Balla, P.; Sinha, A.; Wu, L.; Lu, X.; Tan, D.; Chen, J. Co_3O_4 nanoparticles supported mesoporous carbon framework interface for glucose biosensing. *Talanta* **2019**, *203*, 112–121. [CrossRef]
78. Yao, C.; Ou, J.; Tang, J.; Yang, D. DNA Supramolecular Assembly on Micro/Nanointerfaces for Bioanalysis. *Acc. Chem. Res.* **2022**, *55*, 2043–2054. [CrossRef]
79. Li, F.; Li, Q.; Zuo, X.; Fan, C. DNA framework-engineered electrochemical biosensors. *Sci. China Life Sci.* **2020**, *63*, 1130–1141. [PubMed]
80. Su, S.; Ma, J.; Xu, Y.; Pan, H.; Zhu, D.; Chao, J.; Weng, L.; Wang, L. Electrochemical Analysis of Target-Induced Hairpin-Mediated Aptamer Sensors. *ACS Appl. Mater. Interfaces* **2020**, *12*, 48133–48139. [CrossRef]
81. Li, M.; Lv, M.; Wang, L.; Fan, C.; Zuo, X. Engineering electrochemical interface for biomolecular sensing. *Curr. Opin. Electrochem.* **2019**, *14*, 71–80.
82. Zhu, C.; Liu, D.; Li, Y.; Ma, S.; Wang, M.; You, T. Hairpin DNA assisted dual-ratiometric electrochemical aptasensor with high reliability and anti-interference ability for simultaneous detection of aflatoxin B1 and ochratoxin A. *Biosens. Bioelectron.* **2021**, *174*, 112654.
83. Miao, P.; Tang, Y.; Wang, L. DNA Modified Fe_3O_4@Au Magnetic Nanoparticles as Selective Probes for Simultaneous Detection of Heavy Metal Ions. *ACS Appl. Mater. Interfaces* **2017**, *9*, 3940–3947. [CrossRef]
84. Han, C.; Li, W.; Li, Q.; Xing, W.; Luo, H.; Ji, H.; Fang, X.; Luo, Z.; Zhang, L. CRISPR/Cas12a-Derived electrochemical aptasensor for ultrasensitive detection of COVID-19 nucleocapsid protein. *Biosens. Bioelectron.* **2022**, *200*, 113922.
85. Su, J.; Liu, W.; Chen, S.; Deng, W.; Dou, Y.; Zhao, Z.; Li, J.; Li, Z.; Yin, H.; Ding, X.; et al. A Carbon-Based DNA Framework Nano-Bio Interface for Biosensing with High Sensitivity and a High Signal-to-Noise Ratio. *ACS Sens.* **2020**, *5*, 3979–3987. [CrossRef]
86. Mao, X.; Mao, D.; Chen, T.; Jalalah, M.; Al-Assiri, M.S.; Harraz, F.A.; Zhu, X.; Li, G. DNA Hydrogel-Based Three-Dimensional Electron Transporter and Its Application in Electrochemical Biosensing. *ACS Appl. Mater. Interfaces* **2020**, *12*, 36851–36859. [CrossRef]
87. Cui, M.; Gong, Y.; Du, M.; Wang, K.; Li, T.; Zhu, X.; Wang, S.; Luo, X. An antifouling electrochemical biosensor based on a protein imprinted hydrogel for human immunoglobulin G recognition in complex biological media. *Sens. Actuators B Chem.* **2021**, *337*, 129820. [CrossRef]
88. Berezovski, M.; Krylov, S.N. Using DNA-binding proteins as an analytical tool. *J. Am. Chem. Soc.* **2003**, *125*, 13451–13454. [CrossRef]
89. Campuzano, S.; Pedrero, M.; Pingarrón, J.M. Viral protein-based bioanalytical tools for small RNA biosensing. *Trends Analyt. Chem.* **2016**, *79*, 335–343.
90. Quijano-Rubio, A.; Yeh, H.W.; Park, J.; Lee, H.; Langan, R.A.; Boyken, S.E.; Lajoie, M.J.; Cao, L.; Chow, C.M.; Miranda, M.C.; et al. De novo design of modular and tunable protein biosensors. *Nature* **2021**, *591*, 482–487.
91. Wei, Y.; Zeng, Q.; Hu, Q.; Wang, M.; Tao, J.; Wang, L. Self-cleaned electrochemical protein imprinting biosensor basing on a thermo-responsive memory hydrogel. *Biosens. Bioelectron.* **2018**, *99*, 136–141. [CrossRef]
92. Wei, Y.; Zeng, Q.; Huang, J.; Guo, X.; Wang, L.; Wang, L. Preparation of Gas-Responsive Imprinting Hydrogel and Their Gas-Driven Switchable Affinity for Target Protein Recognition. *ACS Appl. Mater. Interfaces* **2020**, *12*, 24363–24369. [CrossRef]
93. Kerry, R.G.; Ukhurebor, K.E.; Kumari, S.; Maurya, G.K.; Patra, S.; Panigrahi, B.; Majhi, S.; Rout, J.R.; del Pilar Rodriguez-Torres, M.; Das, G. A comprehensive review on the applications of nano-biosensor-based approaches for non-communicable and communicable disease detection. *Biomater. Sci.* **2021**, *9*, 3576–3602.
94. Qi, P.; Wan, Y.; Zhang, D. Impedimetric biosensor based on cell-mediated bioimprinted films for bacterial detection. *Biosens. Bioelectron.* **2013**, *39*, 282–288.

95. Jiang, H.; Jiang, D.; Liu, X.; Yang, J. A self-driven PET chip-based imprinted electrochemical sensor for the fast detection of Salmonella. *Sens. Actuators B Chem.* **2021**, *349*, 130785. [CrossRef]
96. Benson, V.S.S.a.D.E. Protein Design Provides Lead(II) Ion Biosensors for Imaging Molecular Fluxes around Red Blood Cells. *Biochemistry* **2009**, *48*, 462–470.
97. Chen, C.; Liu, Y.; Gu, H.-Y. Cellular biosensor based on red blood cells immobilized on Fe_3O_4 Core/Au Shell nanoparticles for hydrogen peroxide electroanalysis. *Microchim. Acta* **2010**, *171*, 371–376. [CrossRef]
98. Liu, J.M.; Zhang, D.D.; Fang, G.Z.; Wang, S. Erythrocyte membrane bioinspired near-infrared persistent luminescence nanocarriers for in vivo long-circulating bioimaging and drug delivery. *Biomaterials* **2018**, *165*, 39–47. [CrossRef]
99. Rostovtsev, V.V.; Green, L.G.; Fokin, V.V.; Sharpless, K.B. A stepwise huisgen cycloaddition process: Copper (I)-catalyzed regioselective "ligation" of azides and terminal alkynes. *Angew. Chem. Int. Ed.* **2002**, *114*, 2708–2711.
100. Rodionov, V.O.; Presolski, S.I.; Díaz Díaz, D.; Fokin, V.V.; Finn, M. Ligand-accelerated Cu-catalyzed azide− alkyne cycloaddition: A mechanistic report. *J. Am. Chem. Soc.* **2007**, *129*, 12705–12712. [CrossRef]
101. Chan, T.R.; Hilgraf, R.; Sharpless, K.B.; Fokin, V.V. Polytriazoles as copper (I)-stabilizing ligands in catalysis. *Org. Lett.* **2004**, *6*, 2853–2855. [CrossRef] [PubMed]
102. Yanez-Sedeno, P.; Gonzalez-Cortes, A.; Campuzano, S.; Pingarron, J.M. Copper(I)-Catalyzed Click Chemistry as a Tool for the Functionalization of Nanomaterials and the Preparation of Electrochemical (Bio)Sensors. *Sensors* **2019**, *19*, 2379. [CrossRef]
103. Nicosia, C.; Huskens, J. Reactive self-assembled monolayers: From surface functionalization to gradient formation. *Mater. Horiz.* **2014**, *1*, 32–45. [CrossRef]
104. Zhang, X.; Wu, Y.; Chen, J.; Yang, Y.; Li, G. Bioinspired Artificial "Clickase" for the Catalytic Click Immunoassay of Foodborne Pathogens. *Anal. Chem.* **2021**, *93*, 3217–3225. [CrossRef]
105. Guerrero, S.; Cadano, D.; Agüí, L.; Barderas, R.; Campuzano, S.; Yáñez-Sedeño, P.; Pingarrón, J.M. Click chemistry-assisted antibodies immobilization for immunosensing of CXCL7 chemokine in serum. *J. Electroanal. Chem.* **2019**, *837*, 246–253. [CrossRef]
106. Fomo, G.; Nwaji, N.; Nyokong, T. Low symmetric metallophthalocyanine modified electrode via click chemistry for simultaneous detection of heavy metals. *J. Electroanal. Chem.* **2018**, *813*, 58–66.
107. Genzer, J.; Bhat, R.R. Surface-bound soft matter gradients. *Langmuir* **2008**, *24*, 2294–2317. [PubMed]
108. Yang, L.; Gao, M.X.; Zou, H.Y.; Li, Y.F.; Huang, C.Z. Plasmonic $Cu_{2-x}S_ySe_{1-y}$ Nanoparticles Catalyzed Click Chemistry Reaction for SERS Immunoassay of Cancer Biomarker. *Anal. Chem.* **2018**, *90*, 11728–11733. [CrossRef] [PubMed]
109. Xue, L.; Yang, Y.; Wu, S.; Huang, Y.; Li, J.; Xiang, Y.; Li, G. In Situ Reduction of Porous Copper Metal-Organic Frameworks for Three-Dimensional Catalytic Click Immunoassay. *Anal. Chem.* **2020**, *92*, 2972–2978. [CrossRef]
110. Xiang, W.; Zhang, Z.; Weng, W.; Wu, B.; Cheng, J.; Shi, L.; Sun, H.; Gao, L.; Shi, K. Highly sensitive detection of carcinoembryonic antigen using copper-free click chemistry on the surface of azide cofunctionalized graphene oxide. *Anal. Chim. Acta* **2020**, *1127*, 156–162. [CrossRef]
111. Lutz, J.F. Copper-free azide-alkyne cycloadditions: New insights and perspectives. *Angew. Chem. Int. Ed.* **2008**, *47*, 2182–2184. [CrossRef]
112. Agard, N.J.; Prescher, J.A.; Bertozzi, C.R. A strain-promoted [3+2] azide− alkyne cycloaddition for covalent modification of biomolecules in living systems. *J. Am. Chem. Soc.* **2004**, *126*, 15046–15047. [CrossRef] [PubMed]
113. Yang, J.; Wang, K.; Zhang, S.; Zheng, X.; Cui, T.; Yang, X.; Liu, Y.; Lu, D.; Wang, Y.; Tian, X.; et al. Site-Specific Introduction of Bioorthogonal Handles to Nanopores by Genetic Code Expansion. *Angew. Chem. Int. Ed.* **2023**, *62*, 202216115. [CrossRef] [PubMed]
114. Toulemon, D.; Pichon, B.P.; Leuvrey, C.d.; Zafeiratos, S.; Papaefthimiou, V.; Cattoën, X.; Bégin-Colin, S. Fast assembling of magnetic iron oxide nanoparticles by microwave-assisted copper (I) catalyzed alkyne–azide cycloaddition (CuAAC). *Chem. Mater.* **2013**, *25*, 2849–2854. [CrossRef]
115. Cintas, P.; Barge, A.; Tagliapietra, S.; Boffa, L.; Cravotto, G. Alkyne–azide click reaction catalyzed by metallic copper under ultrasound. *Nat. Prot.* **2010**, *5*, 607–616. [CrossRef]
116. Tasdelen, M.A.; Yagci, Y. Light-induced click reactions. *Angew. Chem. Int. Ed.* **2013**, *52*, 5930–5938. [CrossRef] [PubMed]
117. Qi, H.; Li, M.; Zhang, R.; Dong, M.; Ling, C. Double electrochemical covalent coupling method based on click chemistry and diazonium chemistry for the fabrication of sensitive amperometric immunosensor. *Anal. Chim. Acta* **2013**, *792*, 28–34. [CrossRef]
118. Devaraj, N.K.; Dinolfo, P.H.; Chidsey, C.E.; Collman, J.P. Selective functionalization of independently addressed microelectrodes by electrochemical activation and deactivation of a coupling catalyst. *J. Am. Chem. Soc.* **2006**, *128*, 1794–1795. [CrossRef]
119. Lesniewski, A.; Matyjewicz, J.; Palys, B.; Niedziolka-Jonsson, J. Electroassisted click chemistry immobilisation of gold nanoparticles on a solid substrate. *Electrochem. Commun.* **2015**, *53*, 20–23. [CrossRef]
120. Villalba, M.; Bossi, M.; Pozo, M.D.; Calvo, E.J. Palladium Nanoparticles Embedded in a Layer-by-Layer Nanoreactor Built with Poly(Acrylic Acid) Using "Electro-Click Chemistry". *Langmuir* **2016**, *32*, 6836–6842. [CrossRef]
121. Yamamoto, T.; Akahori, M.; Natsui, K.; Saitoh, T.; Einaga, Y. Controlled decoration of boron-doped diamond electrodes by electrochemical click reaction (e−CLICK). *Carbon* **2018**, *130*, 350–354. [CrossRef]
122. Rydzek, G.; Jierry, L.; Parat, A.; Thomann, J.S.; Voegel, J.C.; Senger, B.; Hemmerle, J.; Ponche, A.; Frisch, B.; Schaaf, P.; et al. Electrochemically triggered assembly of films: A one-pot morphogen-driven buildup. *Angew. Chem. Int. Ed.* **2011**, *50*, 4374–4377. [CrossRef]

123. Hu, L.; Zhao, P.; Deng, H.; Xiao, L.; Qin, C.; Du, Y.; Shi, X. Electrical signal guided click coating of chitosan hydrogel on conductive surface. *RSC Adv.* **2014**, *4*, 13477. [CrossRef]
124. Cheng, C.; Oueslati, R.; Wu, J.; Chen, J.; Eda, S. Capacitive DNA sensor for rapid and sensitive detection of whole genome human herpesvirus-1 dsDNA in serum. *Electrophoresis* **2017**, *38*, 1617–1623. [CrossRef]
125. Castiello, F.R.; Porter, J.; Modarres, P.; Tabrizian, M. Interfacial capacitance immunosensing using interdigitated electrodes: The effect of insulation/immobilization chemistry. *Phys. Chem. Chem. Phys.* **2019**, *21*, 15787–15797. [CrossRef] [PubMed]
126. Cesbron, M.; Levillain, E.; Breton, T.; Gautier, C. Click chemistry: A versatile method for tuning the composition of mixed organic layers obtained by reduction of diazonium cations. *ACS Appl. Mater. Interfaces* **2018**, *10*, 37779–37782. [CrossRef]
127. Cernat, A.; Griveau, S.; Martin, P.; Lacroix, J.C.; Farcau, C.; Sandulescu, R.; Bedioui, F. Electrografted nanostructured platforms for click chemistry. *Electrochem. Commun.* **2012**, *23*, 141–144. [CrossRef]
128. Fenoy, G.E.; Hasler, R.; Quartinello, F.; Marmisolle, W.A.; Lorenz, C.; Azzaroni, O.; Bauerle, P.; Knoll, W. "Clickable" Organic Electrochemical Transistors. *JACS Au* **2022**, *2*, 2778–2790. [CrossRef] [PubMed]
129. Sciortino, F.; Rydzek, G.; Grasset, F.; Kahn, M.L.; Hill, J.P.; Chevance, S.; Gauffre, F.; Ariga, K. Electro-click construction of hybrid nanocapsule films with triggered delivery properties. *Phys. Chem. Chem. Phys.* **2018**, *20*, 2761–2770. [CrossRef]
130. Guerrero, S.; Agui, L.; Yanez-Sedeno, P.; Pingarron, J.M. Design of electrochemical immunosensors using electro-click chemistry. Application to the detection of IL-1beta cytokine in saliva. *Bioelectrochemistry* **2020**, *133*, 107484. [CrossRef]
131. Wei, T.; Dong, T.; Xing, H.; Liu, Y.; Dai, Z. Cucurbituril and Azide Cofunctionalized Graphene Oxide for Ultrasensitive Electro-Click Biosensing. *Anal. Chem.* **2017**, *89*, 12237–12243. [CrossRef] [PubMed]
132. Levrie, K.; Jans, K.; Vos, R.; Ardakanian, N.; Verellen, N.; Van Hoof, C.; Lagae, L.; Stakenborg, T. Multiplexed site-specific electrode functionalization for multitarget biosensors. *Bioelectrochemistry* **2016**, *112*, 61–66. [CrossRef]
133. Rydzek, G.; Terentyeva, T.G.; Pakdel, A.; Golberg, D.; Hill, J.P.; Ariga, K. Simultaneous electropolymerization and electro-click functionalization for highly versatile surface platforms. *ACS Nano* **2014**, *8*, 5240–5248. [CrossRef]
134. Chmielarz, P.; Fantin, M.; Park, S.; Isse, A.A.; Gennaro, A.; Magenau, A.J.; Sobkowiak, A.; Matyjaszewski, K. Electrochemically mediated atom transfer radical polymerization (eATRP). *Prog. Polym. Sci.* **2017**, *69*, 47–78. [CrossRef]
135. Wu, T.; Lankshear, E.R.; Downard, A.J. Simultaneous Electro-Click and Electrochemically Mediated Polymerization Reactions for One-Pot Grafting from a Controlled Density of Anchor Sites. *ChemElectroChem* **2019**, *6*, 5149–5154. [CrossRef]
136. Kang, D.; Kim, T.W.; Kubota, S.R.; Cardiel, A.C.; Cha, H.G.; Choi, K.S. Electrochemical Synthesis of Photoelectrodes and Catalysts for Use in Solar Water Splitting. *Chem. Rev.* **2015**, *115*, 12839–12887. [CrossRef]
137. Guiseppi-Elie, A. Electroconductive hydrogels: Synthesis, characterization and biomedical applications. *Biomaterials* **2010**, *31*, 2701–2716. [CrossRef]
138. Nederberg, F.; Trang, V.; Pratt, R.C.; Kim, S.-H.; Colson, J.; Nelson, A.; Frank, C.W.; Hedrick, J.L.; Dubois, P.; Mespouille, L. Exploring the versatility of hydrogels derived from living organocatalytic ring-opening polymerization. *Soft Matter* **2010**, *6*, 2006. [CrossRef]
139. Choi, E.J.; Shin, J.; Khaleel, Z.H.; Cha, I.; Yun, S.-H.; Cho, S.-W.; Song, C. Synthesis of electroconductive hydrogel films by an electro-controlled click reaction and their application to drug delivery systems. *Polym. Chem.* **2015**, *6*, 4473–4478. [CrossRef]
140. Fosdick, S.E.; Knust, K.N.; Scida, K.; Crooks, R.M. Bipolar electrochemistry. *Angew. Chem. Int. Ed.* **2013**, *52*, 10438–10456. [CrossRef]
141. Shida, N.; Zhou, Y.; Inagi, S. Bipolar Electrochemistry: A Powerful Tool for Electrifying Functional Material Synthesis. *Acc. Chem. Res.* **2019**, *52*, 2598–2608. [CrossRef] [PubMed]
142. Shida, N.; Ishiguro, Y.; Atobe, M.; Fuchigami, T.; Inagi, S. Electro-Click Modification of Conducting Polymer Surface Using Cu(I) Species Generated on a Bipolar Electrode in a Gradient Manner. *ACS Macro. Lett.* **2012**, *1*, 656–659. [CrossRef]
143. Zhou, Y.; Shida, N.; Tomita, I.; Inagi, S. Fabrication of Gradient and Patterned Organic Thin Films by Bipolar Electrolytic Micelle Disruption Using Redox-Active Surfactants. *Angew. Chem. Int. Ed.* **2021**, *60*, 14620–14629. [CrossRef]
144. Khan, A.; Khan, A.A.; Asiri, A.M.; Rub, M.A.; Azum, N.; Rahman, M.M.; Khan, S.B.; Ghani, S.A. A new trend on biosensor for neurotransmitter choline/acetylcholine—An overview. *Appl. Biochem. Biotechnol.* **2013**, *169*, 1927–1939. [CrossRef] [PubMed]
145. Wu, J.; Mao, Z.; Tan, H.; Han, L.; Ren, T.; Gao, C. Gradient biomaterials and their influences on cell migration. *Interface Focus* **2012**, *2*, 337–355. [CrossRef] [PubMed]
146. Rydzek, G.; Toulemon, D.; Garofalo, A.; Leuvrey, C.; Dayen, J.F.; Felder-Flesch, D.; Schaaf, P.; Jierry, L.; Begin-Colin, S.; Pichon, B.P.; et al. Selective Nanotrench Filling by One-Pot Electroclick Self-Constructed Nanoparticle Films. *Small* **2015**, *11*, 4638–4642. [CrossRef] [PubMed]
147. Quinton, D.; Maringa, A.; Griveau, S.; Nyokong, T.; Bedioui, F. Surface patterning using scanning electrochemical microscopy to locally trigger a "click" chemistry reaction. *Electrochem. Commun.* **2013**, *31*, 112–115. [CrossRef]
148. Krabbenborg, S.O.; Nicosia, C.; Chen, P.; Huskens, J. Reactivity mapping with electrochemical gradients for monitoring reactivity at surfaces in space and time. *Nat. Commun.* **2013**, *4*, 1667. [CrossRef]
149. Nicosia, C.; Krabbenborg, S.O.; Chen, P.; Huskens, J. Shape-controlled fabrication of micron-scale surface chemical gradients via electrochemically activated copper(i) "click" chemistry. *J. Mater. Chem. B* **2013**, *1*, 5417–5428. [CrossRef]
150. Hansen, T.S.; Daugaard, A.E.; Hvilsted, S.r.; Larsen, N.B. Spatially Selective Functionalization of Conducting Polymers by "Electroclick" Chemistry. *Adv. Mat.* **2009**, *21*, 4483–4486. [CrossRef]

151. Cui, X.; Wei, T.; Hao, M.; Qi, Q.; Wang, H.; Dai, Z. Highly sensitive and selective colorimetric sensor for thiocyanate based on electrochemical oxidation-assisted complexation reaction with Gold nanostars etching. *J. Hazard. Mater.* **2020**, *391*, 122217. [CrossRef]
152. Goll, M.; Ruff, A.; Muks, E.; Goerigk, F.; Omiecienski, B.; Ruff, I.; Gonzalez-Cano, R.C.; Lopez Navarrete, J.T.; Ruiz Delgado, M.C.; Ludwigs, S. Functionalized branched EDOT-terthiophene copolymer films by electropolymerization and post-polymerization "click"-reactions. *Beilstein. J. Org. Chem.* **2015**, *11*, 335–347. [CrossRef] [PubMed]
153. Saylan, Y.; Erdem, O.; Unal, S.; Denizli, A. An Alternative Medical Diagnosis Method: Biosensors for Virus Detection. *Biosensors* **2019**, *9*, 65. [CrossRef] [PubMed]
154. Ku, S.-Y.; Wong, K.-T.; Bard, A.J. Surface patterning with fluorescent molecules using click chemistry directed by scanning electrochemical microscopy. *J. Am. Chem. Soc.* **2008**, *130*, 2392–2393. [CrossRef] [PubMed]
155. Coceancigh, H.; Tran-Ba, K.H.; Siepser, N.; Baker, L.A.; Ito, T. Longitudinally Controlled Modification of Cylindrical and Conical Track-Etched Poly(ethylene terephthalate) Pores Using an Electrochemically Assisted Click Reaction. *Langmuir* **2017**, *33*, 11998–12006. [CrossRef]
156. Rydzek, G.; Polavarapu, P.; Rios, C.; Tisserant, J.-N.; Voegel, J.-C.; Senger, B.; Lavalle, P.; Frisch, B.; Schaaf, P.; Boulmedais, F.; et al. Morphogen-driven self-construction of covalent films built from polyelectrolytes and homobifunctional spacers: Buildup and pH response. *Soft Matter* **2012**, *8*, 10336. [CrossRef]
157. Chatterjee, A.K.; Chakraborty, R.; Basu, T. Mechanism of antibacterial activity of copper nanoparticles. *Nanotechnology* **2014**, *25*, 135101. [CrossRef]
158. Yang, M.; Jalloh, A.S.; Wei, W.; Zhao, J.; Wu, P.; Chen, P.R. Biocompatible click chemistry enabled compartment-specific pH measurement inside *E. coli*. *Nat. Commun.* **2014**, *5*, 4981. [CrossRef]
159. Cheng, X.; Liu, D.; Jin, Y.; Yang, M.; Xiang, J. Addressing Cu^{2+} interference for accurate aptamer-based biomarker determinations of Alzheimer's disease. *Anal. Sci.* **2022**, *38*, 317–322. [CrossRef]
160. Liu, G.; Gui, S.; Zhou, H.; Zeng, F.; Zhou, Y.; Ye, H. A strong adsorbent for Cu^{2+}: Graphene oxide modified with triethanolamine. *Dalton. Trans.* **2014**, *43*, 6977–6980. [CrossRef]